

Performance analysis of distributed power flow controller with ultra-capacitor for regulating the frequency deviations in restructured power system



K. Peddakapu^a, M.R. Mohamed^{a,*}, M.H. Sulaiman^a, P. Srinivasarao^b, A.S. Veerendra^a, P.K. Leung^c

^a Faculty of Electrical & Electronics Eng., Universiti Malaysia Pahang, Pekan, Malaysia

^b Department of Electrical & Electronic Eng., Nalanda Institute of Eng.&Tech., A.P, India

^c Faculty of Engineering and the Environment, University of Southampton, Highfield, United Kingdom

ARTICLE INFO

Keywords:

Automatic generation control
bat algorithm
facts controllers
ultra-capacitor
2dof controllers
deregulated power system

ABSTRACT

This paper presents a novel approach for automatic generation control (AGC) of two-area deregulated system with unequal sources for sustaining the frequency and tie-line power at perturbations. The combination of ultra-capacitor (UC) and various FACTS controllers such as Thyristor-controlled series capacitor (TCSC), Static synchronous series compensator (SSSC), Unified power flow controller (UPFC), and Distributed power flow controller (DPFC) have been investigated in AGC of interconnected system with thermal-wind and hydro-diesel generating units. An innovative metaheuristic method called bat algorithm (BA) is used to ascertain the optimal gain parameters of the two degree of freedom (2DOF) controllers using an integral squared error (ISE) criteria. Furthermore, the productive assessment of the bat tuned 2DOF controllers are also compared with teaching learning-based optimization (TLBO) and cuckoo search (CS) methods optimized 2DOF in distinct contract scenarios of the suggested restructured system. The effect of the coordinated performance of UC and DPFC has been mitigated the oscillatory response of the AGC system at various operating circumstances. The investigations disclose that the bat optimized 2DOF-PID yield the productive outcomes with coordination of DPFC and UC in all contract transactions of the restructured system.

1. Introduction

The toughest work in an electrical system is to control the interconnected power system in effective manner due to the extensive size of generating units, incorporate the high penetration level of renewable sources, and escalating the utilization of electricity. The privilege of an interconnected system is to sustain an uninterrupted power supply to consumers and improves the system consistency. However, the challengeable assignment in an interconnected system is to stabilize the power production and demand without violating the frequency and voltage. amongst distinct control schemes of power systems [1], automatic generation control (AGC) is a prominent strategy to diminish the fluctuations in frequency and tie-line power at perturbations.

The primary duty of AGC is, to retain the constant frequency, to decline the abrupt disturbances in load, to accomplish a productive dynamic behaviour with regards to settling time, peak overshoot and overshoot, to pretend a prolific protective margin to the system at different non-linearities [2–4]. Nowadays, the number of countries is going to reform their electrical structure from vertically integrated utilities (VIU) to the horizontal type thereby, increasing the competitive nature between the retailers. The objective of the restructured system is to create the competition in business, revitalization of the country's economy, and supply the reliable power to the consumers at low prices.

Fig. 1 demonstrated the transition of traditional electric system into liberalization, it has comprised of various power companies namely, generation-based companies (GENCOs), transmission-based companies

* Corresponding author:

E-mail address: rusllim@ump.edu.my (M.R. Mohamed).

<https://doi.org/10.1016/j.est.2020.101676>

Received 10 April 2020; Received in revised form 3 June 2020; Accepted 10 July 2020

2352-152X/ © 2020 Elsevier Ltd. All rights reserved.

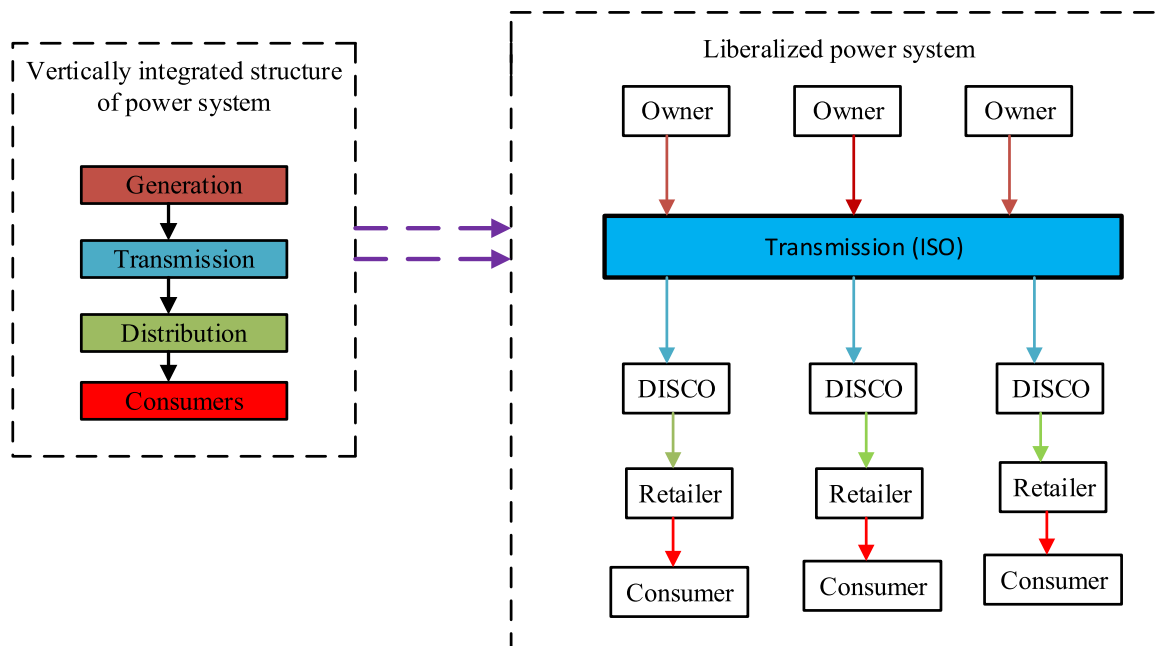


Fig. 1. Transition of traditional power system into liberalization.

(TRANSCOs), and distribution-based companies (DISCOs). The independent system operator (ISO) would monitor the transactions between the power companies without any violation. In addition, various kinds of power transactions are existed in the open market scenario, namely pool-co, bilateral, and agreement violation-based transactions [5]-[6]. The AGC mechanism performs an esteemed role in deregulated system for retaining the scheduled frequency at diverse load circumstances.

So far, several control strategies have been presented in the AGC system for mitigating the frequency fluctuations. Saikia et al. [6], examined the AGC system with the traditional methods like integral derivative (ID), integral double derivative (IDD), proportional integral (PI), and proportional integral derivative (PID) for enhancing the system stability. According to examination by Saikia et al. [6], the IDD controller had given a finer dynamic outcome as compared to other approaches. However, these controllers are not requisite to the vast power system under liberalized environment. Furthermore, a few researchers [7]-[8] initiated the two-degree freedom (2DOF) of PID controllers for solving the obstacles in the AGC system. Sanchez et al. [9], have developed the 2DOF PI strategy in the AGC for enrich the system performance. Even though 2DOF controllers are being evaluated by itself in the conventional power system, these controllers are not still presented in deregulated market with different sources. Therefore, it is required to be evaluated in the AGC system under liberalized environment.

In order to acquire the finest gains of the controllers, appropriate optimization approaches are essential. In recent years, there has been

an increasing amount of literature on computational methods in the AGC of multi-area system with various sources under deregulated system. The optimization methods such as genetic algorithm (GA) [10], particle swarm optimization (PSO) [11], and differential evolution (DE) [12] are developed in the AGC system for acquiring the finest values. Nevertheless, the GA, DE, and PSO algorithms demonstrate the sluggish convergence speed. Besides, bacterial foraging optimization (BFO) [13], firefly algorithm (FA) [14], and cuckoo search [15] approaches are applied in the deregulated system to alleviate the AGC obstacles. Sahu et al. [16] introduced the TLBO technique to tune the gain parameters of the fuzzy and PID controllers for AGC of two area thermal units. Another modern algorithm was suggested by Xin-She Yang [17] named as a bat algorithm. It is a meta-heuristic algorithm and employs as a powerful technique to solving the optimization difficulties in interconnected power system at perturbations. Although there were several researches about the AGC with many optimization methods, limited studies are available on AGC system with bat algorithm in interconnected or isolated systems. Consequently, it is essential to carry out profound research on the AGC difficulties with bat algorithm under restructured environment.

On the other hand, the power electronics devices like FACTS controllers and energy storage systems are implemented in multi-source power system for mitigating the variations in inter-area, and control the power flow [18]-[19]. Series FACTS controllers such as static synchronous series compensator (SSSC) [20] and thyristor-controlled phase shifter (TCPS) [21] are utilized in the multi-area system to damp out the disturbances in tie-line. Moreover, the combination of

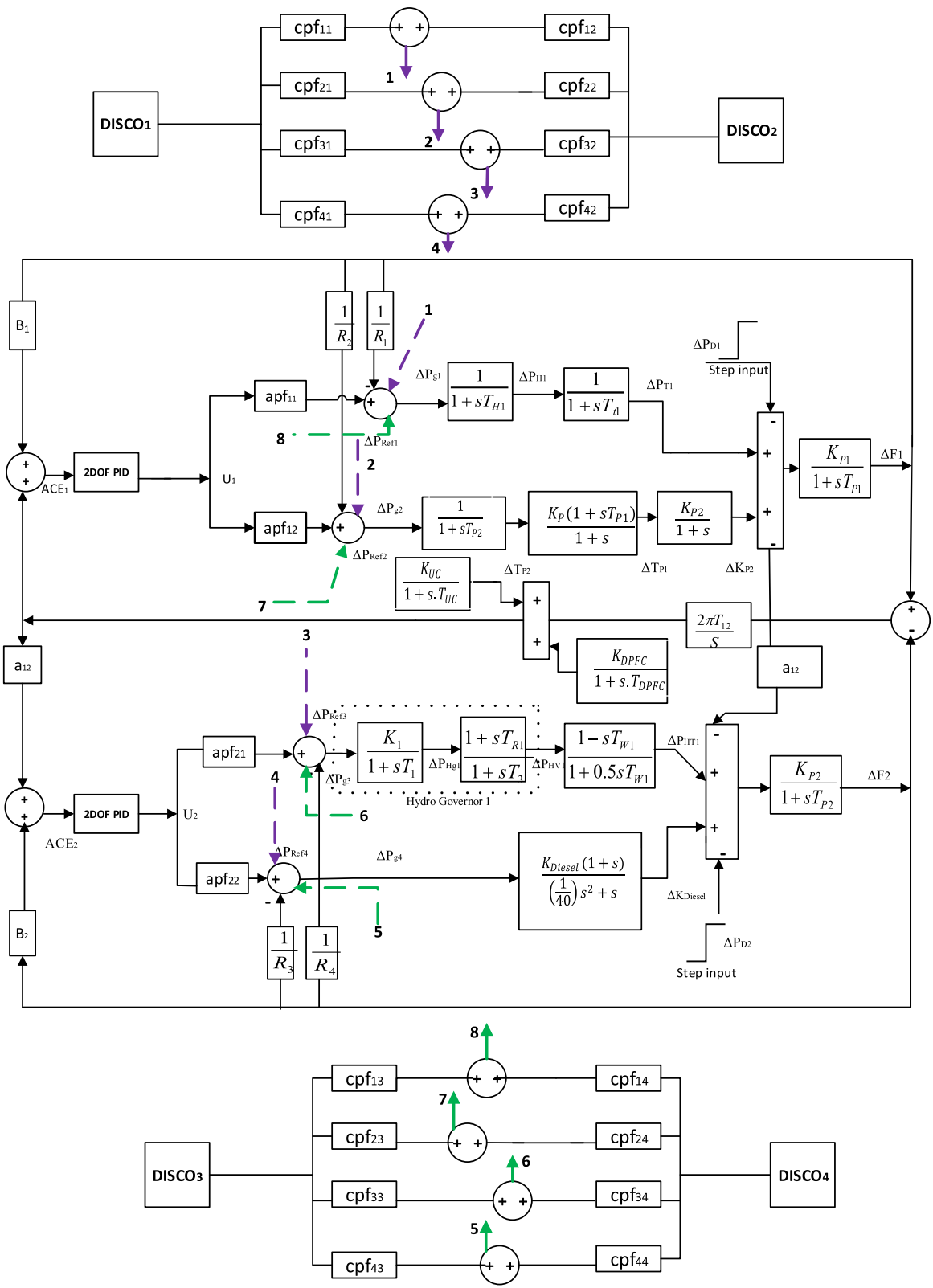


Fig. 2. Two area multi-source power system under liberalized environment.

superconducting magnetic energy storage (SMES) system and TCPS are worked in the AGC of thermal-hydro production units under liberalization [22]. A thyristor-controlled series capacitor (TCSC) is employed in an interconnected system for increasing the power transmitting capability [23]. As the stored capacitors are more economical over gate turn off (GTO) switches, the TCSC is a quite privilege than SSSC in terms of cost and quick response.

Another notable FACT device is unified power flow controller (UPFC), which is interconnected to the tie-line in the form of series for mitigating the unnecessary oscillations. Sahu R.K et al. [24]. adopted the coordination of UPFC and redox flow batteries (RFB) in the liberalized AGC system using hybrid DE and pattern search (PS) algorithm. Nevertheless, RFB would be difficult to locate in every area of multi-area system frequently due to economic considerations. One of the advanced controllers in FACTS devices is distributed power flow controller (DPFC) and resembles UPFC in functioning. However, the price of the UPFC is an extensive than DPFC as well as if any one of the elements can be damaged in UPFC then the whole system would be shut down automatically. It should be noted from the above literatures, however, that few investigations are available on the amalgamation of FACTS controllers and energy storage devices for improving the system performance. amongst limited studies, so far, no attempt was done to explore the potential of DPFC in restructured system with UC. Hence, it is significant to be examined in the AGC of multi-area diverse source restructured system for alleviating the fluctuations in tie-line.

In view of above considerations, the aim of this work is to determine the following:

- 1 To design the two area four-units deregulated system with diverse sources such as thermal, wind, hydro, and diesel.
- 2 To illustrate the supremacy of the bat optimized 2DOF-PID controller than cuckoo and TLBO tuned 2DOF-PID/2DOF-PI/PID under liberalized environment.

- 3 To conduct the comparative study of dynamic performance of the system with the combination of ultra-capacitor and FACTS controllers namely, DPFC, UPFC, SSSC, and TCSC.
- 4 Eventually, to show the productive performance of bat optimized 2 DOF-PID approach with the combination of DPFC and ultra-capacitor over other techniques.

2. System design

The AGC of two-area system with distinct sources under liberalized scenario is addressed in this literature. The block diagram of the two-area with dissimilar sources of restructuring system is shown in Fig. 2. Area 1 consists of thermal (GENCO 1) and wind (GENCO 2) power stations with two DISCOs, which are DISCO 1 and DISCO 2. Likewise, area 2 contains hydro (GENCO 3) and diesel power (GENCO 4) units with DISCO 3 and DISCO 4. The information of each generating unit is yielded in appendix [18] [25]. The overall transfer function model of the suggested system after deregulation is expressed below:

Power system model is represented [18]-[19] as:

$$G_{PS}(s) = \frac{K_{PS}}{1 + s. T_{PS}} \tag{1}$$

For thermal plant [18]-[19],

Speed governor model is:

$$G_{TG}(s) = \frac{1}{1 + s. T_{g1}} \tag{2}$$

Steam turbine model is:

$$G_{TT}(s) = \frac{1}{1 + s. T_{t1}} \tag{3}$$

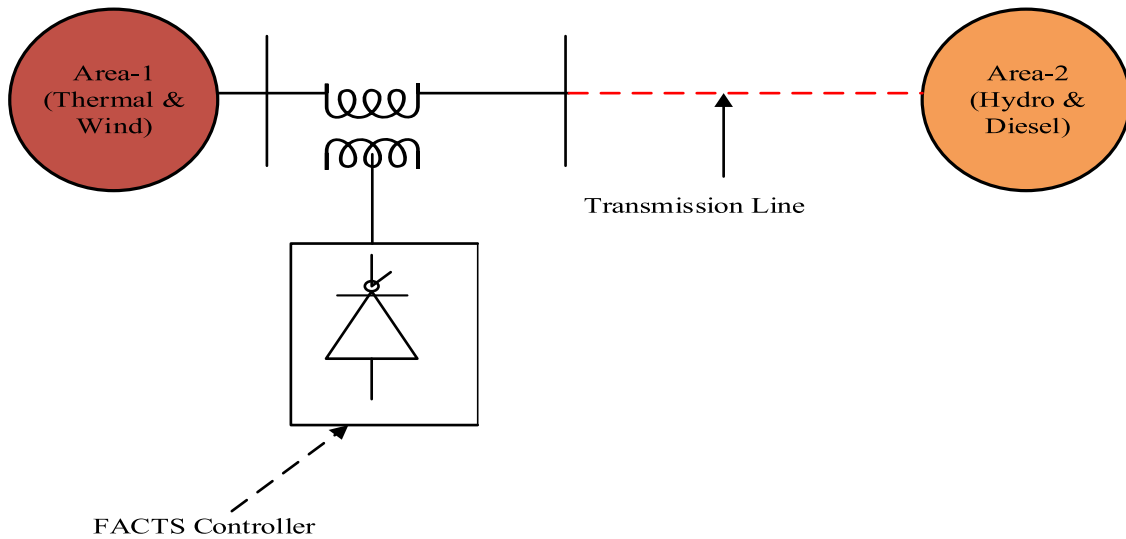


Fig. 3. Schematic arrangement of two area system with FACTS controller.

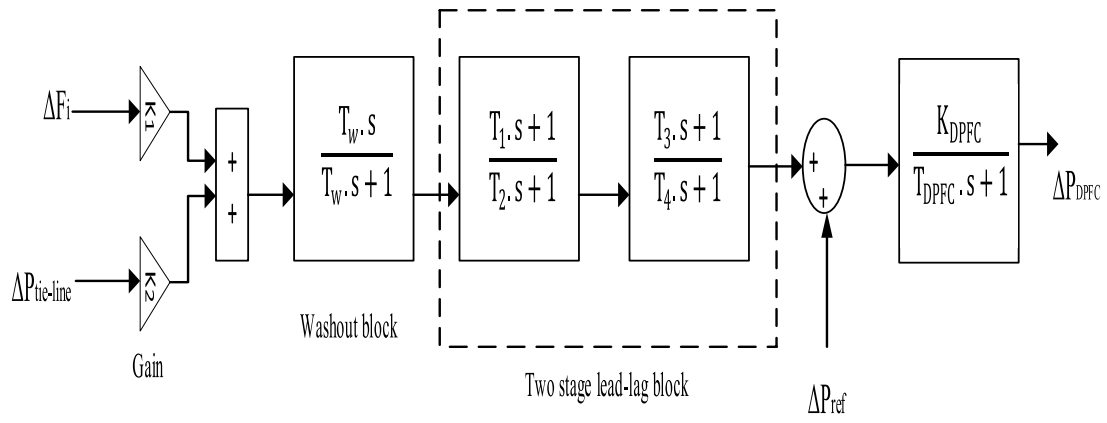


Fig. 4. Structure of the DPFC controller.

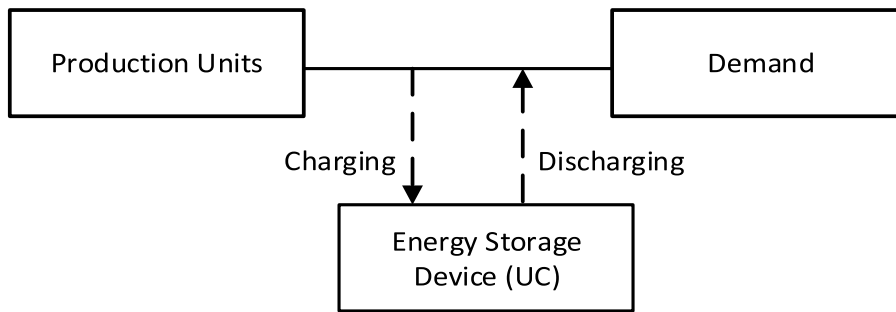


Fig. 5. The basic diagram of the UC in the interconnected system.

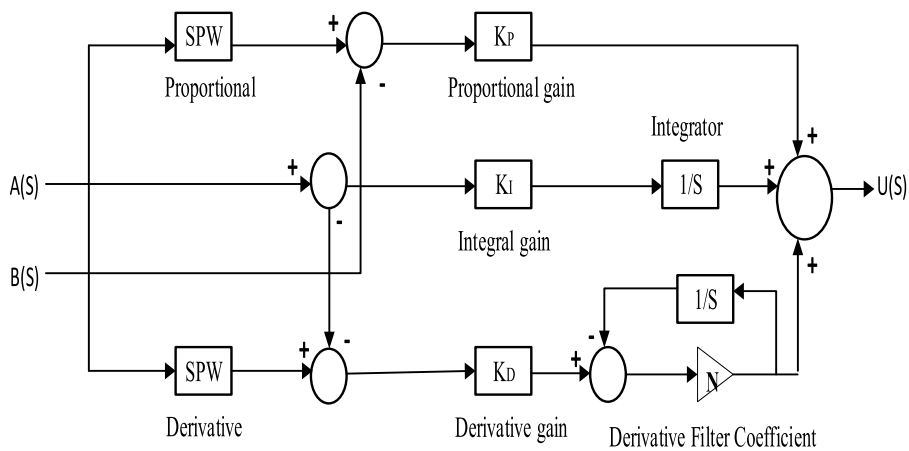


Fig. 6. Block diagram of 2 DOF-PID controller.

For wind plant [18]-[19],
Wind turbine model is:

$$G_{WT}(s) = \frac{1}{1 + s \cdot T_{p2}} \quad (4)$$

Transfer function of drive train is:

$$G_{DT}(s) = \left[\frac{K_p(1 + s \cdot T_{p1})}{1 + s} \cdot \frac{K_{p2}}{1 + s} \right] \quad (5)$$

For hydro plant [18]-[19],

Transfer function of mechanical hydraulic governor is:

$$G_{HG}(s) = \left[\frac{K_1}{1 + s \cdot T_{t1}} \right] \left[\frac{1 + s \cdot T_{R1}}{1 + s \cdot T_3} \right] \quad (6)$$

Transfer function of hydro turbine is:

$$G_{HT}(s) = \left[\frac{1 - s \cdot T_{w1}}{1 + 0.5 s \cdot T_{w1}} \right] \quad (7)$$

For diesel plant [18],

Transfer function of diesel governor is:

$$G_{DG}(s) = \frac{1}{1 + s \cdot T_{gd}} \quad (8)$$

Transfer function of diesel generator is:

$$G_{DGen}(s) = \frac{1}{1 + s \cdot T_{td}} \quad (9)$$

Furthermore, in this work, equal participation factors (apf_{11} & apf_{12}) are considered for thermal and wind plants as 0.5 in area 1 whereas, for hydro and diesel (apf_{21} & apf_{22}) units, which is assumed as 0.5. Subsequently, various controllers such as 2DOF PID, 2DOF PI, and PID are treated as secondary controllers in the AGC system. In addition, different FACTS controllers like DPFC, UPFC, SSSC, and TCSC are introduced in the proposed system in the presence of the ultra-capacitor. The gain constants of the recommended controllers are tuned by bat, TLBO, and cuckoo search optimization approaches.

Different transactions of agreements between GENCOs and DISCOs are evaluated by the subject of DISCO participation matrix (DPM) [12]-[15], and it is mentioned in (10).

$$DPM = \begin{bmatrix} cpf_{11} & cpf_{12} & cpf_{13} & cpf_{14} \\ cpf_{21} & cpf_{22} & cpf_{23} & cpf_{24} \\ cpf_{31} & cpf_{32} & cpf_{33} & cpf_{34} \\ cpf_{41} & cpf_{42} & cpf_{43} & cpf_{44} \end{bmatrix} \quad (10)$$

From above matrix, the row of a DPM link to GENCOs and columns indicates the DISCOs agreement power.

The scheduled power flow between two areas [12]-[15] is:

$$\Delta P_{tie12,scheduled} = \sum_{i=1}^2 \sum_{j=3}^4 cpf_{ij} \Delta P_{dj} - \sum_{j=3}^4 \sum_{i=1}^2 cpf_{ij} \Delta P_{dj} \quad (11)$$

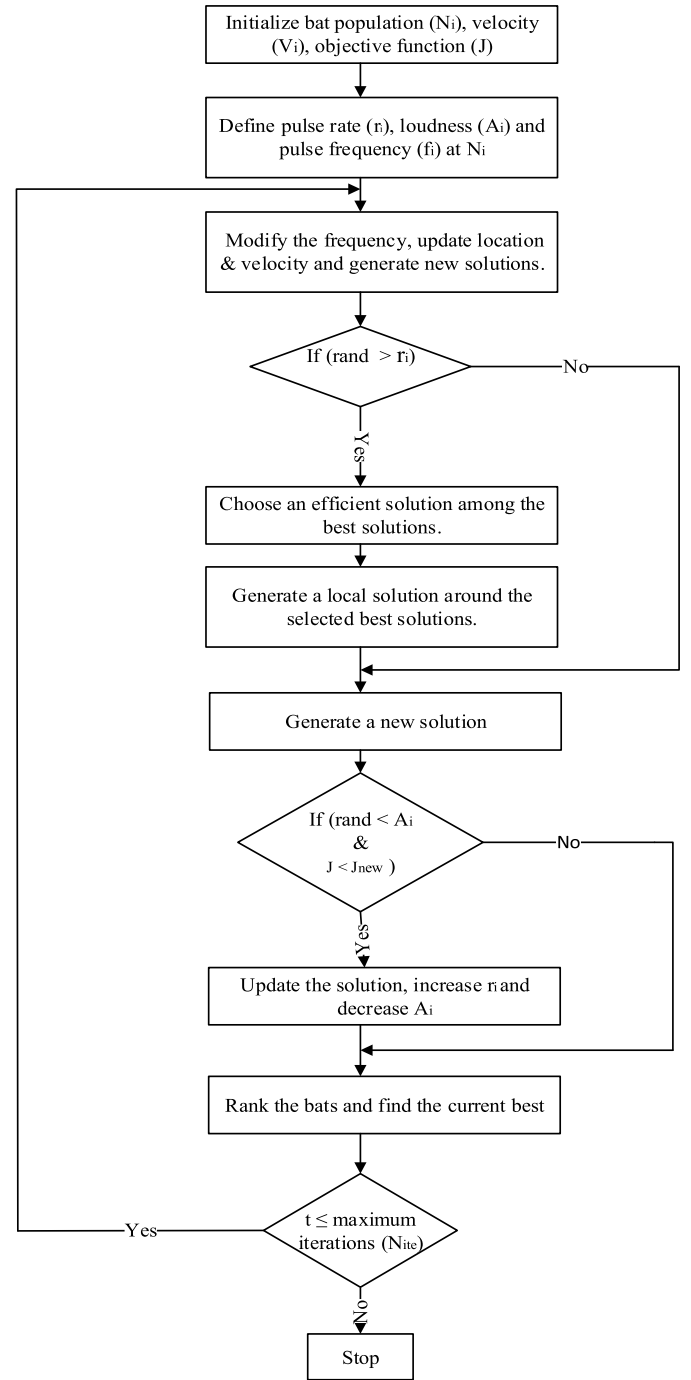


Fig. 7. Flowchart of bat algorithm.

Here cpf is the contract participation factor, and ΔP_D is the load demand of each DISCO.

Equ. (11) can be expanded as:

$$\Delta P_{tie12,schd} = (cpf_{13} + cpf_{23})\Delta P_{d3} + (cpf_{14} + cpf_{24})\Delta P_{d4} - (cpf_{31} + cpf_{41})\Delta P_{d1} - (cpf_{32} + cpf_{42})\Delta P_{d2} \quad (12)$$

The actual inter area power [12]-[15] is:

$$\Delta P_{tie12,actual} = \frac{2\pi T_{12}}{S} (\Delta F_1 - \Delta F_2) \quad (13)$$

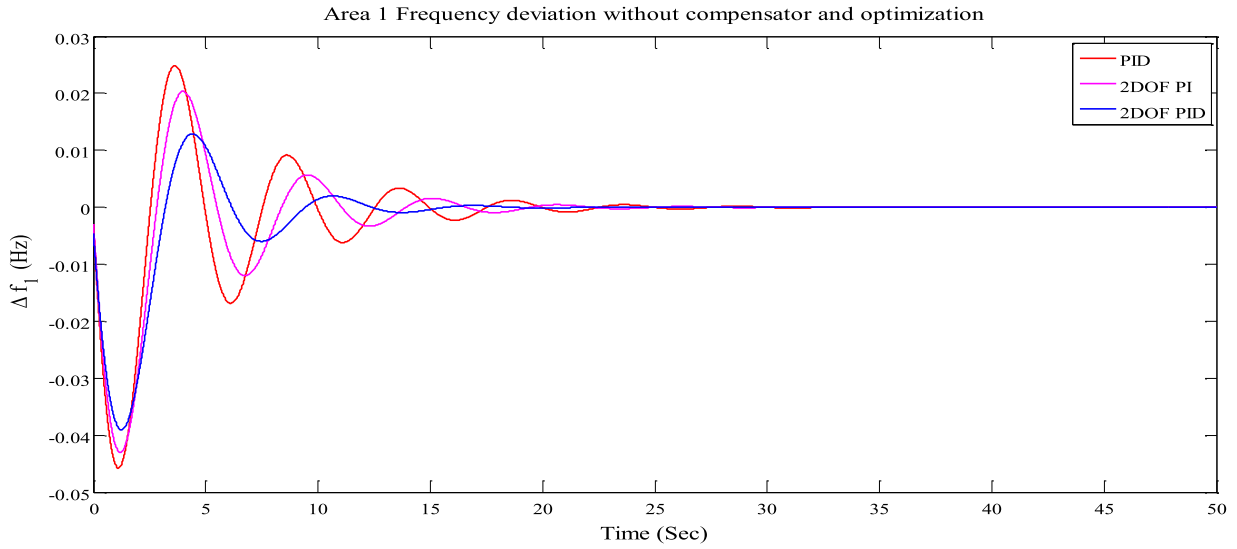
At any instant, the error between two areas is determined using Equ. (14):

$$\Delta P_{tie12,error} = \Delta P_{tie12,actual} - \Delta P_{tie12,scheduled} \quad (14)$$

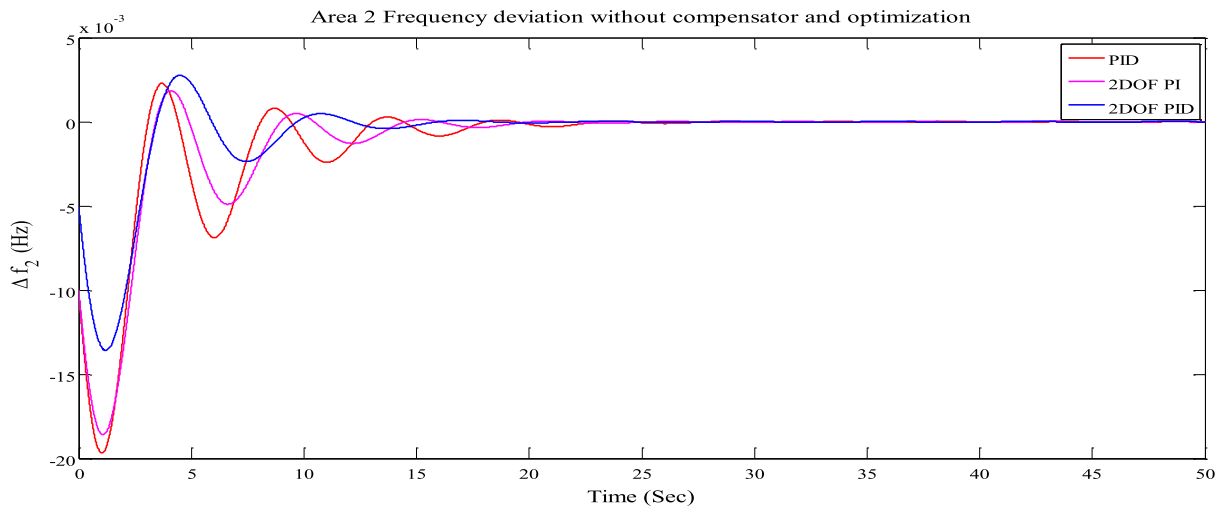
From (14), an error in tie-line power is employed as produced the area control error (ACE) signal in AGC of multi-area system.

ACE is defined as the sum of frequency and error in tie-line [12]-[15].

$$c_1(t) = ACE_1 = \Delta P_{tie12,error} + B_1\Delta F_1 \quad (15)$$



(a)



(b)

Fig. 8. Area 1 and 2 frequency variations with suggested controllers.

$$c_2(t) = ACE_2 = \Delta P_{tie12,error} + B_2 \Delta F_2 \quad (16)$$

$$\text{Where } B_1 = \frac{1}{R_1} + D_1, B_2 = \frac{1}{R_2} + D_2 \quad (17)$$

R_1, R_2 are the speed regulation constants of the two areas, as well as D_1, D_2 are generator damping coefficients.

GENCOs are supplied the incremental power and it can be written as [12]-[15]:

$$\sum_{DISCO=4}^{j=1} cpf_{ij} X \Delta P_{dj} \quad (18)$$

The above Equ. (18) can be expanded as:

$$\begin{aligned} \Delta P_{gi} = & cpf_{i1} X \Delta P_{DISCO1} + cpf_{i2} X \Delta P_{DISCO2} + cpf_{i3} X \Delta P_{DISCO3} \\ & + cpf_{i4} X \Delta P_{DISCO4} \end{aligned} \quad (19)$$

When considering the contract violation [21],

$$\begin{aligned} \Delta P_{gi} = & (cpf_{i1}, DISCO_1) + (cpf_{i2}, DISCO_2) \\ & + (cpf_{i3}, DISCO_3) (cpf_{i1}, DISCO_1) + (cpf_{i2}, DISCO_2) \\ & + (cpf_{i3}, DISCO_3) \end{aligned} \quad (20)$$

Also, the demand of area1 is $\Delta P_{d1} = \Delta P_{DISCO1} + \Delta P_{DISCO2}$, area 2 is $\Delta P_{d2} = \Delta P_{DISCO3} + \Delta P_{DISCO4}$.

2.1. Combination of facts and uc in agc

Numerous countries are endeavouring to generate the huge amount power thorough integration of renewable sources. However, the power system operation and control become difficult due to continues variations of renewable power. Moreover, the interconnected tie-lines are typically congested in areas with huge penetration range of renewable sources, which may create to reduce the capability of the tie-line. Therefore, an interconnected power system requires to be upgraded with new control approaches for increasing the consumption of renewable power. The amalgamation of FACTS and energy storage devices are appropriate to strengthen the power flow ability, accurate load management, optimizing the system operational costs and an adequate provision of ancillary services [20] [22].

In this study, the FACTS controllers such as TCSC, SSSC, UPFC, DPFC are employed in the AGC of deregulated system with the co-ordination of UC for enriching the dynamic behaviour of the system. In realistic power system, the FACTS controllers are placed between the areas for mitigating the deviations in tie-line and improve the power transferring capability. Likewise, the UC is able to deliver the energy into the deregulated system for equalizing the power generation and load at abrupt changes in demand. Hence, the combination of UC and FACTS controller are significant in the AGC of restructured system for strengthening the dynamic stability and optimizing the system operational costs. The detailed description of FACTS and UC are described below:

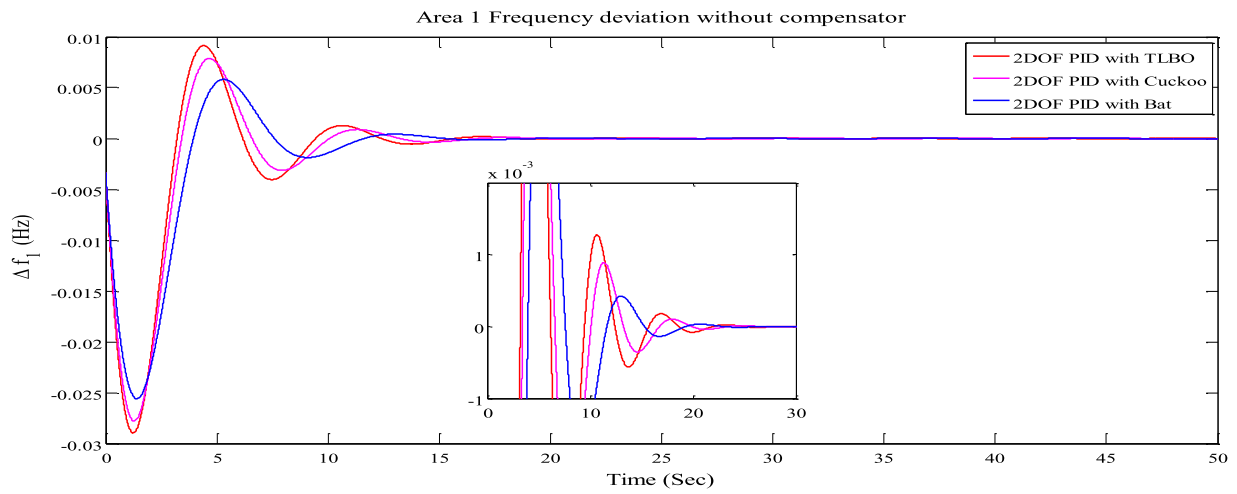
Table 1
Performance analysis of controllers without optimization.

Controller	Response	Parameters	Without optimization
PID	ΔF_1	OS	0.0271
		US	-0.0487
		ST	33.18
2DOF-PI	ΔF_1	OS	0.0214
		US	-0.0432
		ST	29.20
2DOF-PID	ΔF_1	OS	0.0165
		US	-0.0389
		ST	27.43
PID	ΔF_2	OS	0.0036
		US	-0.0192
		ST	36.25
2DOF-PI	ΔF_2	OS	0.0032
		US	-0.0185
		ST	34.23
2DOF-PID	ΔF_2	OS	0.0035
		US	-0.0145
		ST	29.15

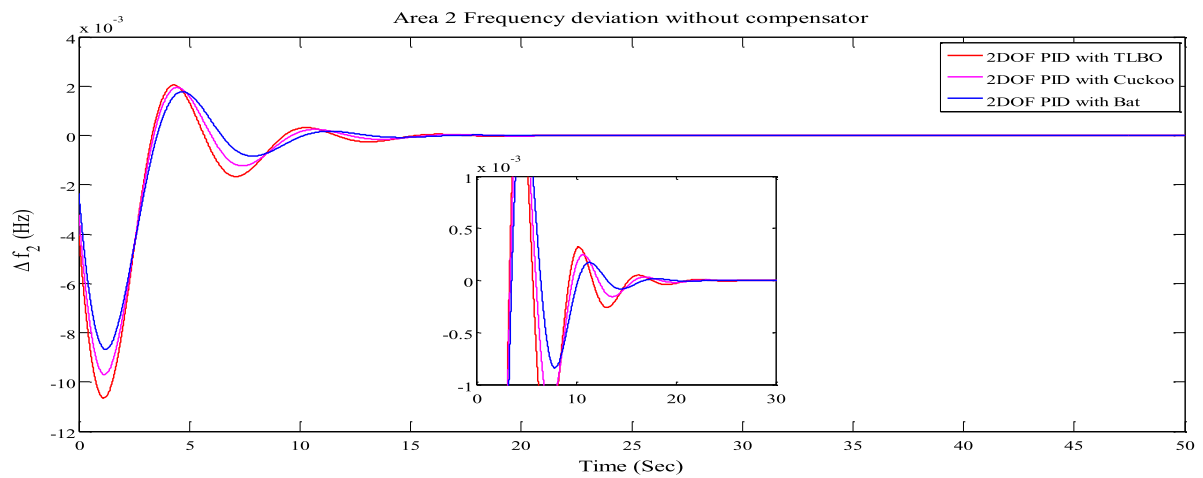
2.1.1. Modelling of facts controller

In this study, different kinds of FACTS controllers namely, SSSC, TCSC, UPFC, and DPFC are used to diminish the deviations in tie-line power and enhances the system dynamic stability. Fig. 3 demonstrates the schematic arrangement of two area system with FACTS controller. TCSC is a great device in interconnected system for regulating the power transfer, and which is connected to the line in cascade way. In addition to stabilize the changes in tie-line power by altering the phase angle of TCSC [23]. Another FACTS device is SSSC, it is also linked to the line in series. The privilege of the SSSC is to supply the voltage in the line continuously thereby, alleviating the voltage drops in line quickly [26]. It should be noted that the SSSC does not only intensify the power flow abilities but also descent it.

Conversely, UPFC performs a significant role in power system for mitigating the changes in tie-line power at distinct disturbances [24]. Moreover, it has the ability to refrain the power transfer between the areas. Nevertheless, the UPFC needs high cost for installing and desires direct current (DC) link to transmit the real power between the converters. Hence, a novel method for transmitting the real power without help of DC link is required. One of the advanced FACTS controllers is DPFC, it is appropriate to multi-area system for enriching the dynamic behaviour of the system. The functioning of the DPFC is resembled to UPFC and can be transferred the real power between the converters without presence of DC link capacitor. Another privilege of DPFC is to maintain continuous power supply with assist of converters even if any one of the converters fails.



(a)



(b)

Fig. 9. Frequency and tie-line power variations with three optimization approaches.

Table 2
Parameters of the suggested algorithms.

Algorithm	Parameters	Quantity
TLBO	Population	40
	No. Generations (N)	100
	Iteration number (obtained optimized values)	80
CS	No. Nests	25
	Discovery rate of alien eggs/solutions	0.25
	No. Generations	100
BA	Iteration number (obtained optimized values)	60
	Population size	40
	No. Generations	100
	Iteration number (obtained optimized values)	30
	Loudness	0.5
	Pulse rate	0.5

Table 3
Dynamic analysis of 2DOF-PID controller with three optimizations.

Method	Response	OS	US	ST	ISE
TLBO-2DOF PID	ΔF_1	0.0093	-00,293	25.21	0.4515
	ΔF_2	0.0019	-0.0104	26.54	
	ΔP_{tie}	0.0048	-0.0152	23.31	
CS-2DOF PID	ΔF_1	0.0079	-0.0274	23.41	0.2248
	ΔF_2	0.0018	-0.0098	24.12	
	ΔP_{tie}	0.0032	-0.0148	22.24	
BAT-2DOF PID	ΔF_1	0.0052	-0.0261	21.10	0.1072
	ΔF_2	0.0016	-0.0083	21.18	
	ΔP_{tie}	0.0025	-0.0137	19.52	

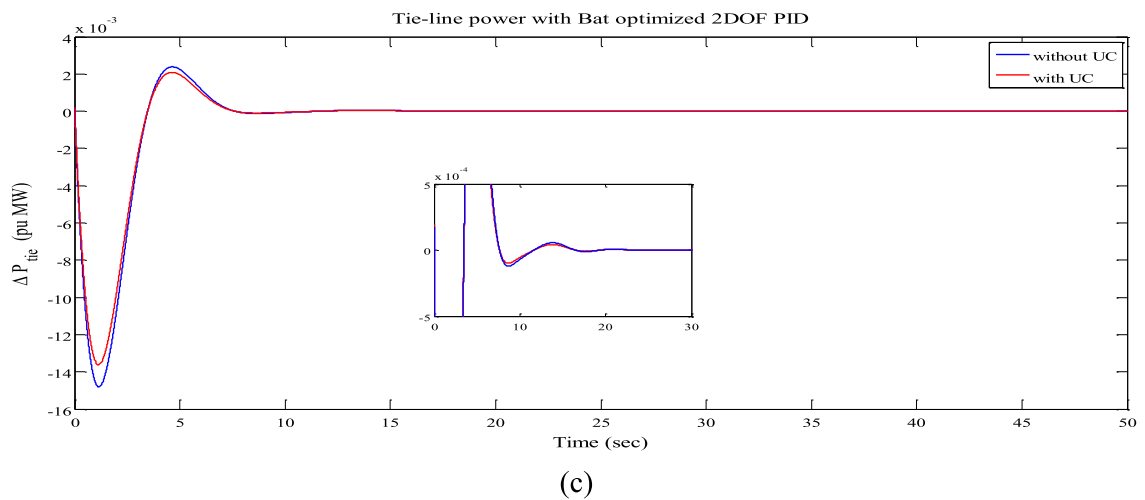
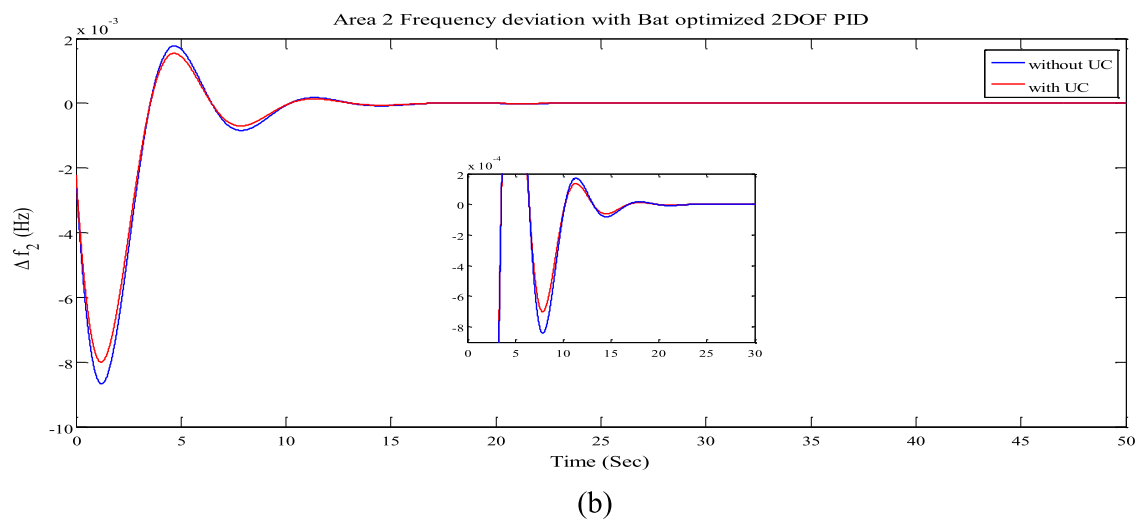
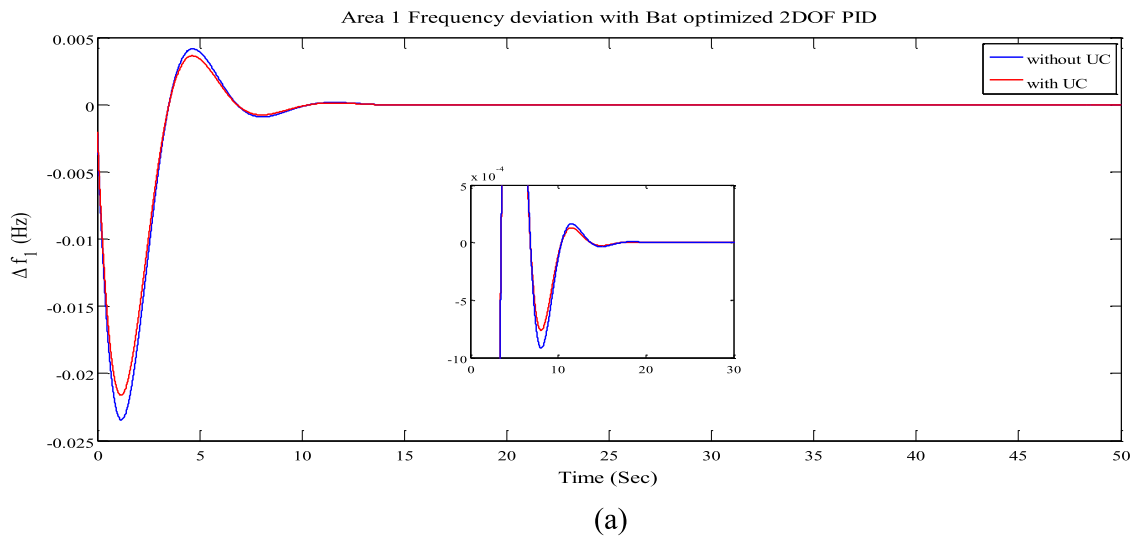


Fig. 10. The deviations of frequency and tie-line power with only UC.

Further, the active power controller of DPFC has a structure of lead-lag compensator with resultant signal (ΔP_{ref}). In this work, the dynamic characteristics of DPFC is designed as first order model with time constant (T_{DPFC}). The power fluctuation of two areas system is injected to the DPFC (ΔP_{DPFC}) and it performs positively for area 1 and negatively for area 2. Hence, the deviated power (ΔP_{DPFC}) move into two areas with positive (+) and negative (-) signs simultaneously. The arrangement of DPFC with lead-lag compensator is demonstrated in Fig. 4. It has been consisted with various blocks such as gain block, washout block and two-stage phase compensation block. In this regard, the gain block is utilized to determine the amount of damping as well as the washout block is more appropriate to diminish the fluctuations at uncertainties. Finally, two-stage phase compensation block contributes suitable phase-lead characteristics for compensating the phase lag between input and output signals. Frequency (ΔF_i) and tie-line power ($\Delta P_{tie-line}$) fluctuations are acted as input signals to the suggested DPFC controller. The parameters of the DPFC such as T_{DPFC} , T_1 , T_2 , T_3 and T_4 are to be tuned by bat algorithm for obtaining optimal design and stabilize the deviations in frequency.

The transfer functions model of the DPFC controllers [21]-[24] is shown below:

$$G_{DPFC} = \frac{K_{DPFC}}{1 + s \cdot T_{DPFC}} \cdot \Delta F_i(s) \quad (21)$$

Similarly, for other FACTS devices are [21]-[24]:

$$G_{TCSC}(s) = \frac{K_{TCSC}}{1 + s \cdot T_{TCSC}} \cdot \Delta F_i(s) \quad (22)$$

$$G_{SSSC}(s) = \frac{K_{SSSC}}{1 + s \cdot T_{SSSC}} \cdot \Delta F_i(s) \quad (23)$$

$$G_{UPFC}(s) = \frac{K_{UPFC}}{1 + s \cdot T_{UPFC}} \cdot \Delta F_i(s) \quad (24)$$

2.1.2. Modelling of ultra-capacitor (UC)

The challengeable task in an interconnected system is to stabilize the oscillations in frequency and inter-area line power as a result of changes in load abruptly and different types of non-linear loads. In addition, the governor is unable to interpret the alterations in frequency due to sluggish response and uncertainties exists in the system. Consequently, the energy storage device such as an ultra-capacitor (UC) is proposed in this restructured system for mitigating the fluctuations in frequency. Another name of UC is supercapacitor, it works on the theory of double layer for maintaining the kinetic energy. The UCs are great power density energy storage devices (ESDs) that store energy electrostatically by polarizing an electrolytic solution. They use high surface area electrode materials (3000 m²/g) and thin electrolytic dielectrics to obtain greater capacitances over traditional capacitors. Furthermore, no need to provide more maintenance and has an extensive lifespan. In this study, two UC units are connected in area 1 and area 2 for mitigating the frequency fluctuations and illustrated in Fig. 2. The changes in frequency

Table 4

Performance analysis of the system with only UC.

BAT-2DOF PID	Response	OS	US	ST	ISE
Without UC	ΔF_1	0.0052	-0.0261	21.10	0.1072
	ΔF_2	0.0016	-0.0083	21.18	
	ΔP_{tie}	0.0025	-0.0137	19.52	
With UC	ΔF_1	0.0047	-0.0232	19.23	0.0875
	ΔF_2	0.0014	-0.0079	19.58	
	ΔP_{tie}	0.0018	-0.0131	18.95	

signals such as ΔF_1 and ΔF_2 are used as input signal for UC to enhance the frequency response. During steady state conditions, the UC gets charged in every area, while the stored energy delivers back to the system during abrupt changes in load. Besides, the UCs can be balanced the generation and load demand at perturbation without violating the system parameters. The basic diagram of the UC in an interconnected system is shown Fig. 5 [19] [22] [24].

Considering diverse assumptions and ignoring non-linearities, the final model of an UC can be represented via a first order lag transfer function [19].

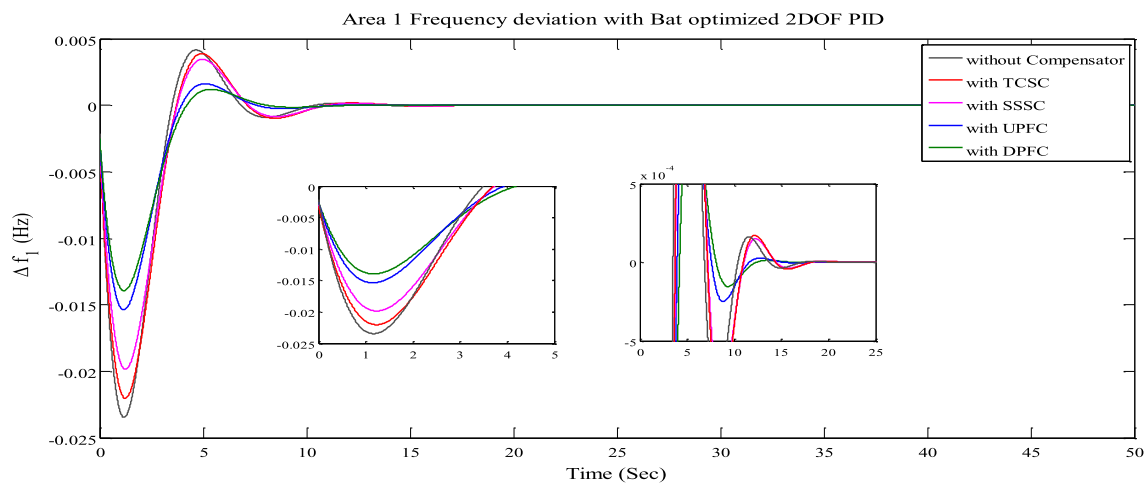
$$G_{UC}(s) = \frac{K_{UCi}}{1 + s \cdot T_{UCi}} \cdot \Delta F_i(s) \quad (25)$$

Where K_{UCi} , T_{UCi} is the gain and time constant of UC respectively. $\Delta F_i(S)$ is the change in frequency signal. K_{UCi} depends on state of charge (SOC), which is the condition at which UC is charged. In this study, K_{UCi} is kept constant at -7/10 between 50 and 90% of operating SOC of UC.

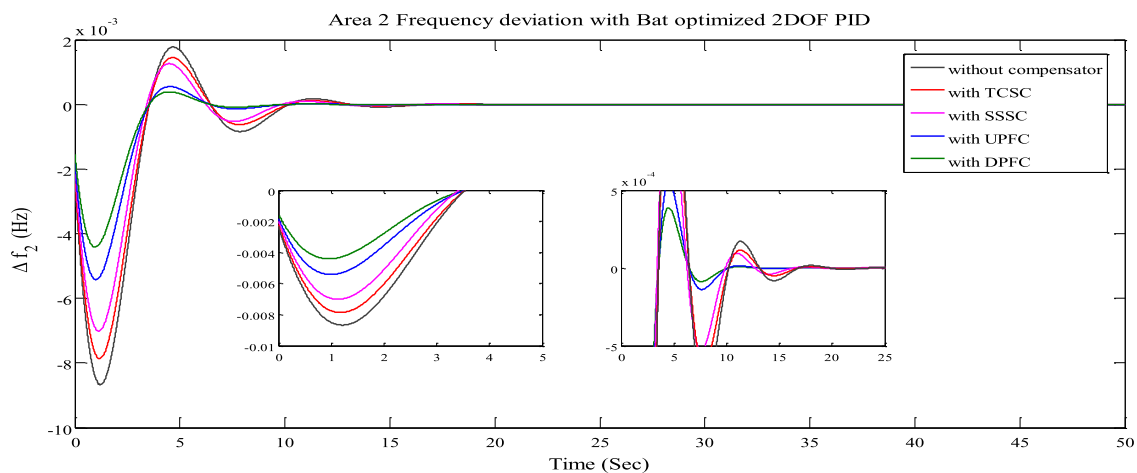
2.2. Design of 2 dof controller

The 2 DOF controllers are being efficient control approaches in control system for solving the non-linear problems, which are adjusted by the traditional controllers. The drawback of conventional controllers is typically not prolific to high order and uncertainties endured systems. Moreover, the control system of 2DOF methods have enormous benefits over single degree freedom of the conventional control system. Since the 2DOF controllers are presented in the system, it can be produced the output signal by using the discrimination between the reference and an evaluated system outcome. The 2DOF controllers have various set point weights on respective proportional, integral, and derivative modes as well as strengthening the system stability [8]. The outcome of the 2DOF controller is the summation of proportional, integral, and derivative endeavours on the corresponding disparity signals.

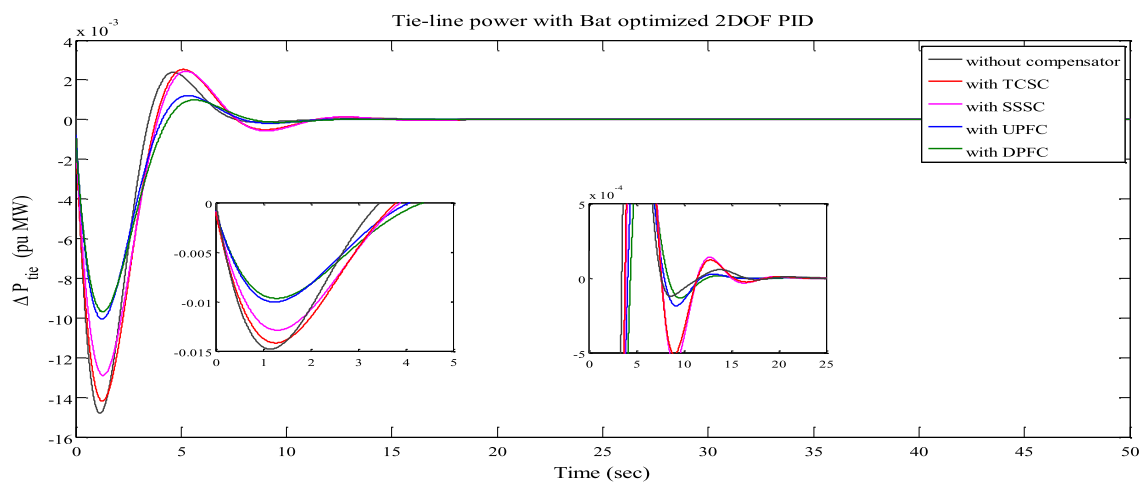
In recent years, many studies have been focused on 2DOF controller implementation in the AGC of multi-area system for minimising the variations in frequency and tie-line powers. The aim of the present study is to investigate the 2DOF controllers such as 2DOF-PI, and 2DOF-PID in the AGC of two areas with different



(a)



(b)



(c)

Fig. 11. The performance of the frequency and tie-line power with only FACTS controllers.

sources under the open market scenario. The block diagram 2DOF-PID controller is depicted in Fig. 6. Further, the gains of the suggested controllers are tuned by TLBO, cuckoo search, and bat optimization approaches.

$$A(S) = bK_p + \frac{K_i}{S} + \frac{cK_d}{T_f S + 1} \quad (26)$$

$$B(S) = - \left[K_p + \frac{K_i}{S} + \frac{K_d}{T_f S + 1} \right] \quad (27)$$

Where $A(S)$ is the system reference signal and $B(S)$ is the estimated signal.

The set points weights (SPW) of the proportional, and derivative controllers are b , c respectively, as well as the gain parameters of the controller are K_p , K_i , K_d . Besides, derivative filter time constant is N .

2.3. Selection of objective function

To sustain the require objectives of the restructured system by optimization approaches, an appropriate objective function is to be selected. Typically, different types of performance indices have been employing in restructured system for designing the controllers with optimization algorithms. Performance indices are integral of time multiplied squared error (ITSE), integral of squared error (ISE), integral of time multiplied absolute error (ITAE), and integral of absolute error (IAE) are used in recent applications of deregulated system [8] [12] [21]. However, the ITSE performance index contributes high controller outcome for an abrupt alter in set point therefore, it is not favourable to design of controller. The drawback of the ITAE indices is to be produced the huge oscillations in response of the system. A weak-point of the IAE indices is that it may bring about a response with a long settling time. Owing to the higher power of the error terms, the ISE indices can alleviate the fluctuations effectively over other performance indices.

In two-area four dissimilar sources of AGC system, per unit (p.u) values of different parameters of the dissimilar areas are considered to be same on their respective MW capacity bases. In addition, the studied two area system has two frequency deviations ($\Delta F_1, \Delta F_2$) and one tie-line power deviation (ΔP_{tie}) whose dynamic response profiles are to be enhanced. In order to enhance these variables, the bat algorithm is applied to tune the 2DOF PID controller gains based on ISE criteria (also referred as figure of demerit (FOD)). It is worked as objective function in this study for minimizing the FOD value within the solution space and it is represented as below [21]:

$$J = \text{FOD} = \int_0^{t_s} [(\Delta F_1)^2 + (\Delta F_2)^2 + (\Delta P_{tie-line})^2].dt \quad (28)$$

Where ΔF_1 , ΔF_2 are the variations in frequency of area 1, 2 and change in tie-line power is represented as $\Delta P_{tie-line}$.

Table 5

Dynamic performance of the system with FACTS only.

BAT-2DOF PID	Response	OS	US	ST	ISE
Without FACTS	ΔF_1	0.0052	-0.0261	21.10	0.1072
	ΔF_2	0.0016	-0.0083	21.18	
	ΔP_{tie}	0.0025	-0.0137	19.52	
With TCSC	ΔF_1	0.0046	-0.0221	19.07	0.0858
	ΔF_2	0.0016	-0.0079	20.24	
	ΔP_{tie}	0.0021	-0.0141	18.95	
With SSSC	ΔF_1	0.0042	-0.0192	18.76	0.0721
	ΔF_2	0.0015	-0.0065	19.85	
	ΔP_{tie}	0.0020	-0.0121	18.23	
With UPFC	ΔF_1	0.0024	-0.0149	15.89	0.0531
	ΔF_2	0.0010	-0.0061	14.76	
	ΔP_{tie}	0.0018	-0.0098	15.14	
With DPFC	ΔF_1	0.0017	-0.0145	14.45	0.0412
	ΔF_2	0.0008	-0.0043	13.52	
	ΔP_{tie}	0.0017	-0.0094	14.87	

2.4. Bat algorithm (BA)

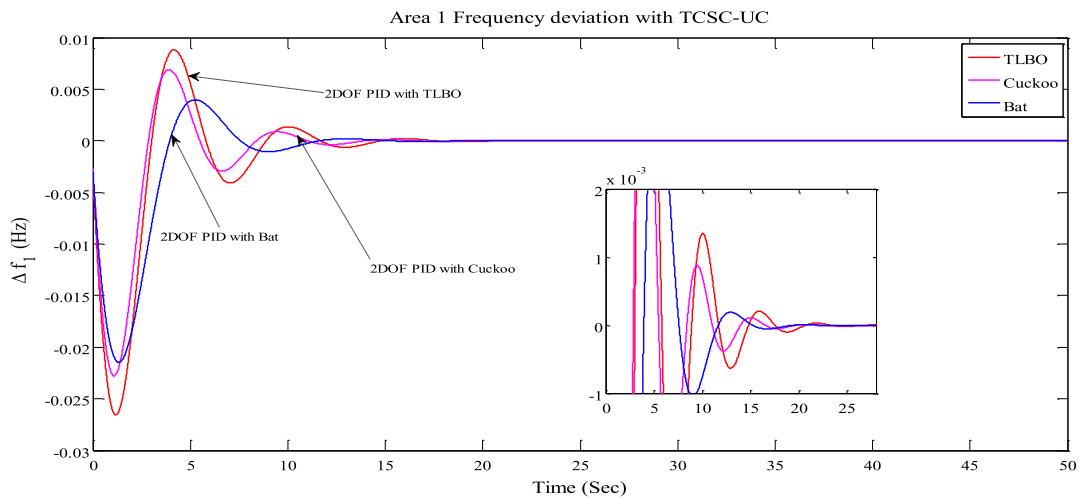
In recent years, there has been growing amount of literature on nature inspired optimization approaches to compute the non-linear problems of power system. One of the new dynamic meta-heuristic techniques is bat algorithm, which was determined by Yang [17]. Bats have great attribute to recognise and avoid the difficulties using sonar echoes, and a flowchart of bat algorithm is shown in Fig. 7. As bats are transmitting the sound signals to various locations for ascertaining the food or prey, those sound pulses are transmuted into useful data for the bats.

Besides, the bats can be navigated itself with the help of time delay from the transmission to the reflection of sound pulses. When bats are hitting or reflecting sound pulses from the object, it would transmute their own sound pulses into productive information to evaluate the distance for food or prey. By using this concept, BA technique is constructed with three idealizing rules such as:

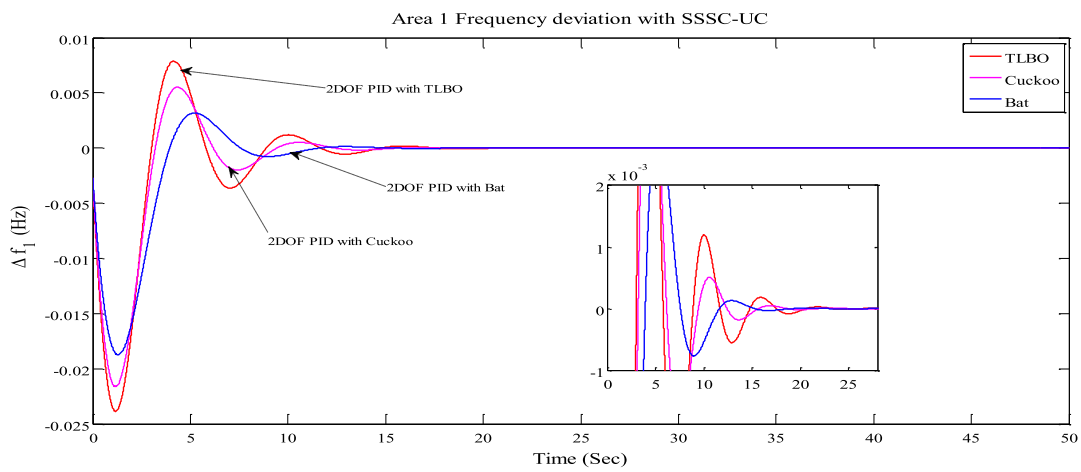
- 1 Every bat adopts echolocation to get the information about distance together with it can be recognized the difference between food or prey and surrounding obstacles.
- 2 Every bat can soar in a random manner with velocity of V_i at location X_i with a minimum frequency f_{min} , changing in wavelength λ , and loudness A_0 is to look for prey. Moreover, bats are not only able to change the wavelength of their transmitted pulses but also manage the rate of sound pulse transmission $r[0, 1]$. Which is completely based on the surrounding target.
- 3 The loudness of the bats is changing from high (A_0) to low values (A_{min}) as they arrive near to target.

2.5. Mathematical formulations

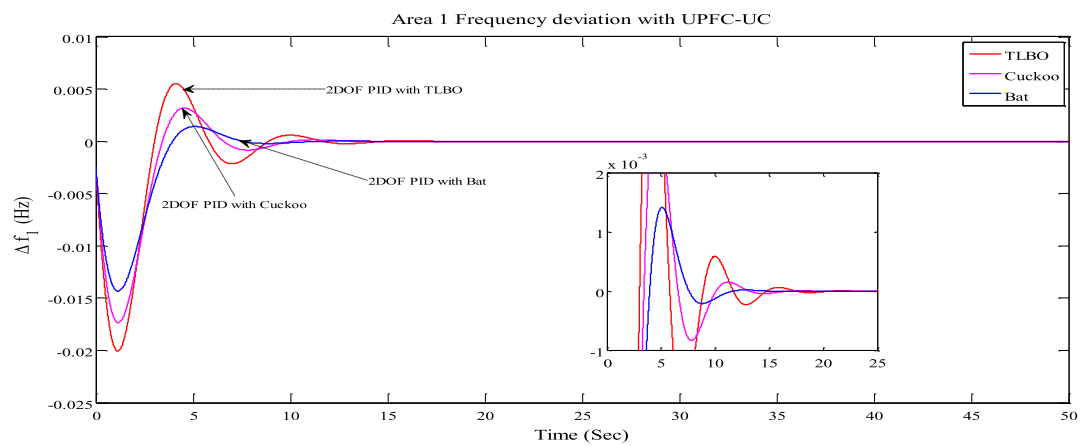
The generation of novel solutions are achieved by virtual bats based



(a)

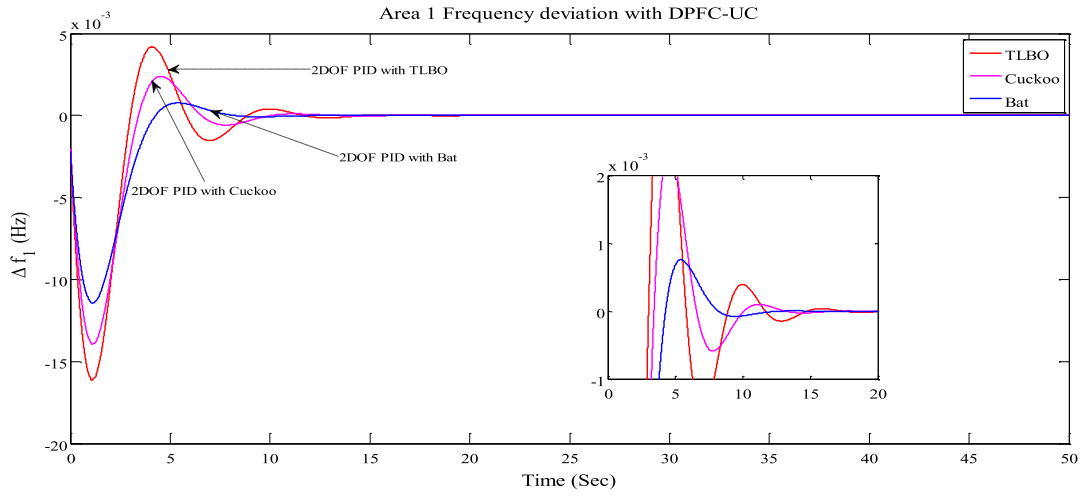


(b)



(c)

Fig. 12. Area 1 frequency variations with the coordination of FACTS controllers and UC.



(d)

Fig. 12. (continued)

on the following equations:

$$f_i = f_{\min} + (f_{\max} - f_{\min})\beta \tag{29}$$

$$V_i^t = V_i^{t-1} + (x_i^t - x^*)f_i \tag{30}$$

$$x_i^t = x_i^{t-1} + V_i^t \tag{31}$$

Here $\beta \in [0, 1]$ is an inconsistent vector taken from a symmetrical distribution. x^* is a new global efficient solution, which is situated when comparing all the locations (solutions) amongst each and every bat.

A new efficient solution for all bats is represented by Equ. (32)

$$x_{\text{new}} = x_{\text{old}} + \partial A^t \tag{32}$$

Where $\partial \in [-1, 1]$ is an inconsistent number, as well as A^t is the mean loudness of all the bats at consider step time.

When the bats are identifying the food or surrounding target, then their loudness will be reduced and shown as:

$$A_i^{t+1} = \alpha \cdot A^t \tag{33}$$

Likewise, the rate of sound pulses will be enhanced when recognize the target by bats.

It can be stated as:

$$r_i^{t+1} = r_i^0 [1 - \exp(-\gamma t)] \tag{34}$$

Where α and γ are the fixed values.

In this work, bat method is applied to tune the gains of 2DOF PID controller for AGC of two-area restructured system. The objective of this algorithm is to develop the finest gain parameters for suggested controller. It is an appropriate to reduce the performance indices

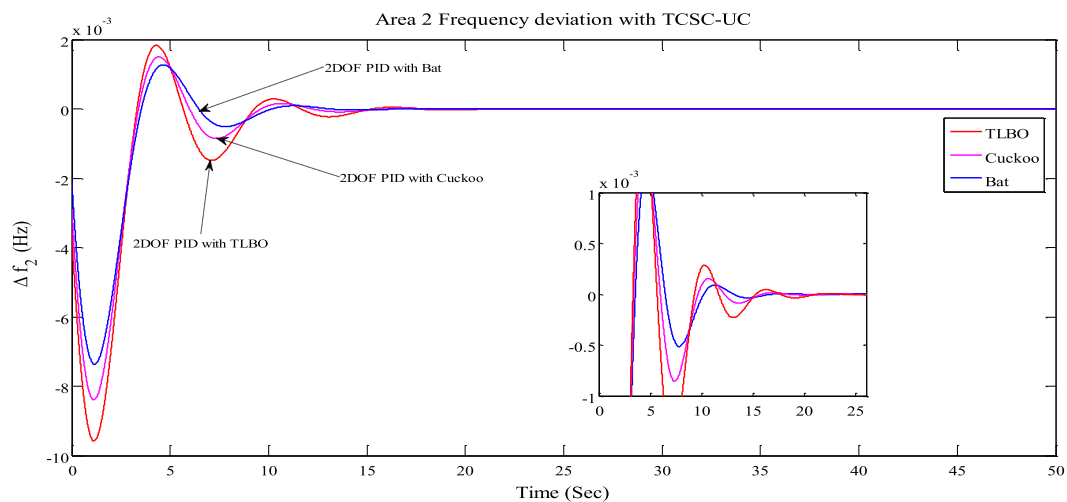
value such as objective function (FOD), which is represented in Equ. (28).

The step by step presentation of the bat algorithm for obtaining the optimal solution can be depicted in following ways:

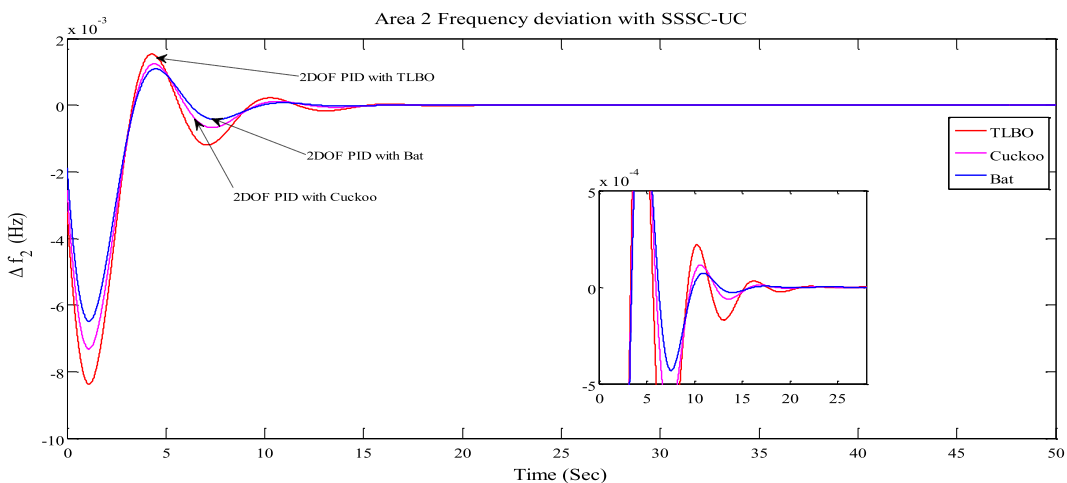
- Step 1: Initialize the bat parameters such as population size (N_i), pulse rate (r_i), loudness (A_i), the maximum amount of iterations (N_{iter}), pulse frequency (f_i) and objective function (J).
- Step 2: Adjust the frequency, update location & velocity and generate new solutions.
- Step 3: Estimate the robustness for every entity in population as stated by objective function.
- Step 4: choose the efficient bat in the population.
- Step 5: upgrade the population of bats.
- Step 6: Verify the termination process and display the finest solutions otherwise return to step 2.

3. Results and discussions

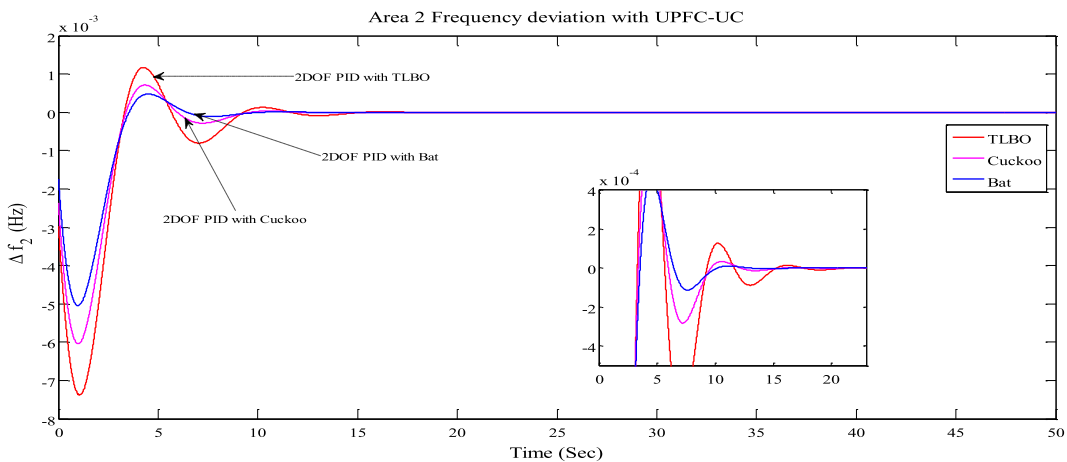
This paper attempts to provide a more detailed investigation regarding the effects of AGC under restructured environment. In this work, the two area multi-sources liberalized system has been studied with different control strategies using optimization techniques such as bat, TLBO and cuckoo search algorithms. The proposed system was designed using MATLAB/Simulink, and demonstrated in Fig. 2. The system specifications are mentioned in appendix. The deregulated system is analysed with three different transactions, namely, pool-co, bilateral, and contract violation.



(a)

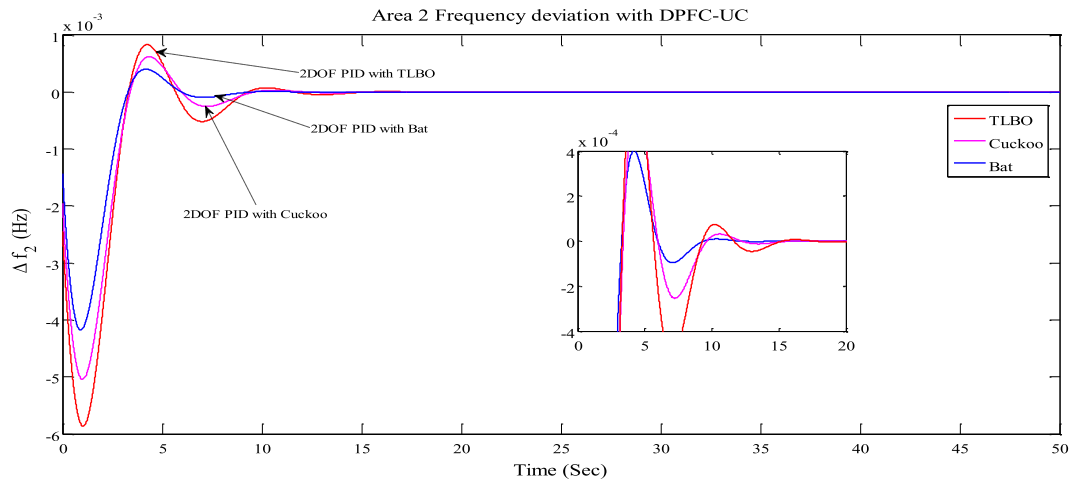


(b)



(c)

Fig. 13. Area 2 frequency variations with the coordination of FACTS controllers and UC.



(d)

Fig. 13. (continued)

3.1. Pool-Co based transaction

In this transaction, DISCOs and GENCOs are having limitations to contract with other areas. With this regard, each area of DISCOs can make an agreement with only that area GENCOs. Area 1 constitutes of two GENCOs and DISCOs, which are GENCO 1, GENCO 2, DISCO 1, and DISCO 2 respectively. Although the demand escalated on DISCOs of area 1, it has to be made a contract with that area (area 1) GENCOs only. Furthermore, ACE participation factors (apf) of every GENCOs yielded as, $apf_{11} = apf_{12} = apf_{21} = apf_{22} = 0.5$. The agreement of DISCOs with GENCOs is shown in Equ.(35).

$$DPM = \begin{bmatrix} 0.6 & 0.7 & 0 & 0 \\ 0.4 & 0.3 & 0 & 0 \\ 0 & 0 & 0 & 0 \\ 0 & 0 & 0 & 0 \end{bmatrix} \tag{35}$$

Variation of all GENCOs generation need to match with all loads of DISCOs, and the required generation of all GENCOs can be calculated using Equ. (19).

For this transaction,

$$\left. \begin{aligned} \Delta P_{G1} &= (0.6*0.1) + (0.7*0.1) + (0*0.1) + (0*0.1) = 0.13 \text{ pu MW} \\ \Delta P_{G2} &= (0.4*0.1) + (0.3*0.1) + (0*0.1) + (0*0.1) = 0.07 \text{ pu MW} \\ \Delta P_{G3} &= \Delta P_{G4} = (0*0.1) + (0*0.1) + (0*0.1) + (0*0.1) = 0 \text{ pu MW} \end{aligned} \right\} \tag{36}$$

Fig. 8(a) depicts the frequency variations in area 1 with PID, 2DOF-PI, and 2DOF-PID controllers. The settling times (ST) of the dynamic response is 33 s for PID, 29 s for 2DOF PI, 27 s for 2DOF-PID. Fig. 8(b) exhibits the fluctuations of frequency in area 2 with suggested controllers. The dynamic analysis of the system has

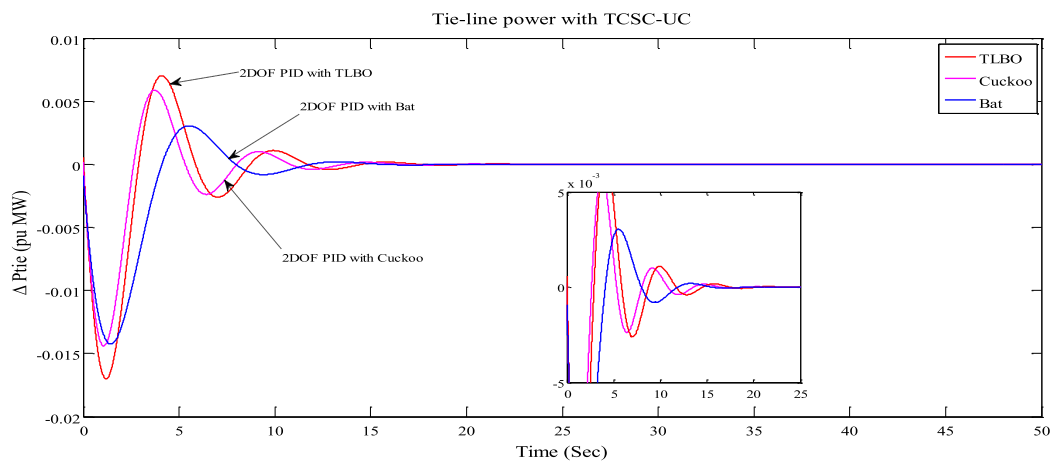
Table 6

The gain values of the 2DOF-PID controller with three algorithms.

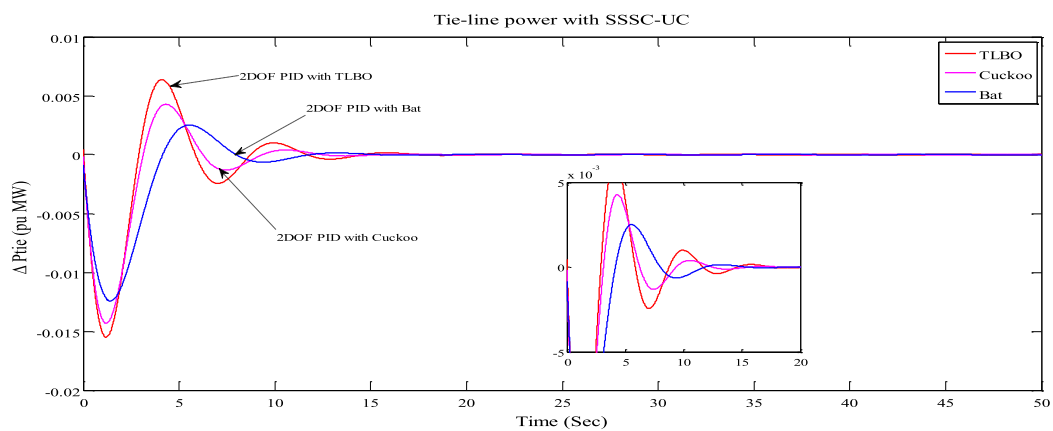
Compensator		Gain values of 2DOF PID	TLBO	Cuckoo	Bat
DPFC-UC	Area 1	K_P	0.8919	0.8996	0.9089
		K_I	0.0031	0.0030	0.0029
		K_D	1.9271	2.0142	2.4732
		b	0.8473	0.1232	0.0947
		c	0.7495	0.1073	0.0617
	N	93.681	92.472	89.324	
	Area 2	K_P	0.9237	0.8893	0.8524
		K_I	0.0046	0.0041	0.0032
		K_D	1.1684	1.4726	1.7324
		b	0.1485	0.1501	0.0992
c		0.2054	0.1726	0.1357	
N	95.416	94.152	88.671		

recorded in Table 1. Based on the simulation results, the 2DOF-PID controller gave finer outcome as compared with other proposed controllers.

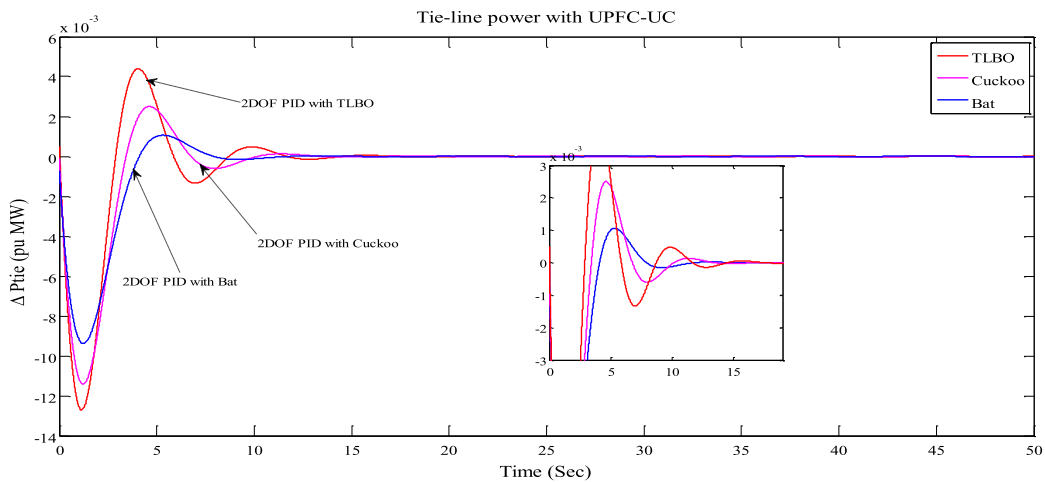
Subsequently, three distinct optimization approaches namely, TLBO, cuckoo search, and bat are introduced to tune the 2DOF-PID controller for obtaining the optimal gain values. Fig. 9(a)-(c) represents the deviations of frequency and tie-line power with 2DOF-PID controller, and which are optimized by TLBO, cuckoo search, and bat algorithms. The parameters of the algorithms [8] [20] are mentioned in Table 2. Besides, the time domain parameters are indicated in Table 3. As per the simulation outcomes in area 1, the settling time



(a)

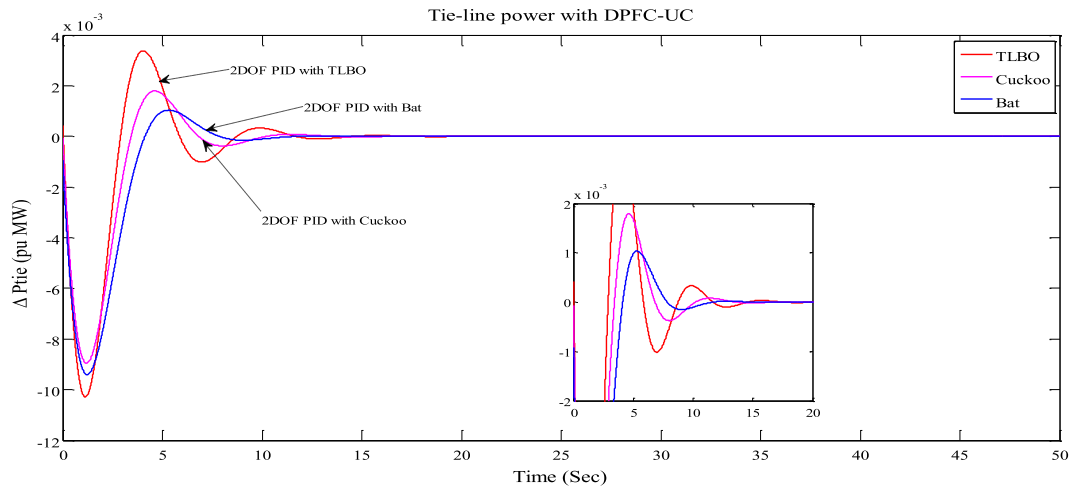


(b)



(c)

Fig. 14. Tie-line power variations with compensators.



(d)

Fig. 14. (continued)

Table 7
Numerical values ST, US, and OS of suggested approaches under pool-co agreement.

Control Approach	Response	OS	US	ST	ISE
TLBO-2DOF-PID-TCSC-UC	ΔF_1	0.0083	-0.0254	23.53	0.262
TLBO-2DOF-PID-TCSC-UC	ΔF_2	0.0018	-0.0098	25.21	
TLBO-2DOF-PID-TCSC-UC	ΔP_{tie}	0.0078	-0.0173	20.72	
Cuckoo-2DOF-PID -TCSC-UC	ΔF_1	0.0069	-0.0223	21.72	0.195
Cuckoo-2DOF-PID -TCSC-UC	ΔF_2	0.0017	-0.0087	23.11	
Cuckoo-2DOF-PID -TCSC-UC	ΔP_{tie}	0.0062	-0.0148	18.54	
Bat-2DOF-PID -TCSC-UC	ΔF_1	0.0041	-0.0218	20.12	0.0795
Bat-2DOF-PID -TCSC-UC	ΔF_2	0.0015	-0.0072	19.54	
Bat-2DOF-PID -TCSC-UC	ΔP_{tie}	0.0042	-0.0133	16.29	
TLBO-2DOF-PID -SSSC-UC	ΔF_1	0.0078	-0.0249	21.85	0.229
TLBO-2DOF-PID -SSSC-UC	ΔF_2	0.0016	-0.0083	22.14	
TLBO-2DOF-PID -SSSC-UC	ΔP_{tie}	0.0069	-0.0168	19.58	
Cuckoo-2DOF-PID -SSSC-UC	ΔF_1	0.0056	-0.0213	20.71	0.121
Cuckoo-2DOF-PID -SSSC-UC	ΔF_2	0.0015	-0.0074	19.58	
Cuckoo-2DOF-PID -SSSC-UC	ΔP_{tie}	0.0048	-0.0142	15.79	
Bat-2DOF-PID -SSSC-UC	ΔF_1	0.0038	-0.0189	18.52	0.062
Bat-2DOF-PID -SSSC-UC	ΔF_2	0.0013	-0.0062	17.43	
Bat-2DOF-PID -SSSC-UC	ΔP_{tie}	0.0037	-0.0129	14.29	
TLBO-2DOF-PID -UPFC-UC	ΔF_1	0.0059	-0.0291	19.76	0.207
TLBO-2DOF-PID -UPFC-UC	ΔF_2	0.0015	-0.0073	20.42	
TLBO-2DOF-PID -UPFC-UC	ΔP_{tie}	0.0042	-0.0135	16.97	
Cuckoo-2DOF-PID -UPFC-UC	ΔF_1	0.0035	-0.0178	17.83	0.089
Cuckoo-2DOF-PID -UPFC-UC	ΔF_2	0.0009	-0.0059	16.51	
Cuckoo-2DOF-PID -UPFC-UC	ΔP_{tie}	0.0027	-0.0112	13.57	
Bat-2DOF-PID -UPFC-UC	ΔF_1	0.0018	-0.0142	14.80	0.042
Bat-2DOF-PID -UPFC-UC	ΔF_2	0.0006	-0.0049	14.28	
Bat-2DOF-PID -UPFC-UC	ΔP_{tie}	0.0018	-0.0085	11.88	
TLBO-2DOF-PID -DPFC-UC	ΔF_1	0.0045	-0.0172	17.27	0.108
TLBO-2DOF-PID -DPFC-UC	ΔF_2	0.0015	-0.0058	18.42	
TLBO-2DOF-PID -DPFC-UC	ΔP_{tie}	0.0038	-0.0109	15.83	
Cuckoo-2DOF-PID -DPFC-UC	ΔF_1	0.0023	-0.0145	15.29	0.045
Cuckoo-2DOF-PID -DPFC-UC	ΔF_2	0.0084	-0.0049	14.83	
Cuckoo-2DOF-PID -DPFC-UC	ΔP_{tie}	0.0022	-0.0085	12.02	
Bat-2DOF-PID -DPFC-UC	ΔF_1	0.0015	-0.0128	12.57	0.036
Bat-2DOF-PID -DPFC-UC	ΔF_2	0.0013	-0.0041	12.41	
Bat-2DOF-PID -DPFC-UC	ΔP_{tie}	0.0015	-0.0088	10.05	

Table 8
Comparative analysis of suggested method with existed techniques.

Controller type	Pool-co based Overshoot (OS)			ISE
	ΔF_1	ΔF_2	ΔP_{tie}	
hTLBO-PS based TID with TCPS-SMES [21]	0.0722	0.0704	0.0035	0.1661
DE-PID [12]	0.0409	0.012	0.0057	0.0548
Proposed method (BAT optimized 2DOF PID with DPFC-UC)	0.0015	0.0013	0.0015	0.0362

Table 9
Gain values of the bat optimized 2DOF-PID with DPFC-UC in three cases.

Gain values of 2DOF PID		DPFC-UC with Bat Optimization		
		Pool-Co	Bilateral	Contract Violation
Area 1	K_P	0.9089	0.9087	0.9088
	K_I	0.0029	0.0029	0.0029
	K_D	2.4732	2.4737	2.4737
	b	0.0947	0.0973	0.0951
	c	0.0617	0.0712	0.0723
Area 2	N	89.324	89.425	89.456
	K_P	0.8524	0.8531	0.8544
	K_I	0.0032	0.0032	0.0032
	K_D	1.7324	1.7319	1.7321
	b	0.0992	0.0997	0.1008
	c	0.1357	0.1534	0.1278
	N	88.671	88.928	88.543

of bat optimized 2DOF PID shows 21.10 s whereas, 23.41 s for CS-2DOF PID, 25.21 s for TLBO-2DOF PID. Likewise, for area 2, bat based 2DOF PID demonstrates 21.18 s, 24.12 s for CS based 2DOF PID and 26.54 s for TLBO based 2DOF PID. For tie-line power, 19.52 s for bat, 22.4 s for cuckoo, and 23.31 s for TLBO. It has been observed that the

bat tuned 2DOF PID controller is mitigated the frequency and tie-line oscillations as quickly over TLBO and CS tuned 2DOF PID. As compared with time performance index, bat based 2DOF PID provides minimum value (ISE=0.1072) than TLBO (ISE=0.2248) and CS (ISE=0.4515).

Further, the suggested two area deregulated system has been integrated with the only energy storage device like UC for increasing the system dynamic stability. The deviations of frequency and tie-line power has observed with and without UC and demonstrated in Fig. 10(a)-(c). The time performance of the system is recorded in Table 4. The results reveal that the bat tuned 2DOF PID with UC yields finer enhancement with respect to settling time (ST), overshoot (OS) and undershoot (US).

Similarly, only FACTS controllers such as TCSC, SSSC, UPFC and DPFC are incorporated with the proposed system and monitored the system dynamic performance. Fig. 11(a)-(c) shows the frequency and tie-line power responses of the system with FACTS controllers in the presence of bat tuned 2DOF PID. The numerical data of ST, US, OS and ISE are reported in Table 5. Based on the results, the bat tuned DPFC gives the productive outcomes and produce less performance indices (ISE=0.0412) value than without FACTS (ISE=0.1072), TCSC (0.0858), SSSC(ISE=0.0721) and UPFC(ISE=0.0531).

In addition, the system has been incorporated with the both ultra-capacitor (UC) and FACTS controllers like SSSC, UPFC, TCSC, and DPFC for improving the system stability. Fig. 12(a)-(d) and Fig. 13(a)-(d) illustrates the fluctuations of frequency in area 1 and 2 with the

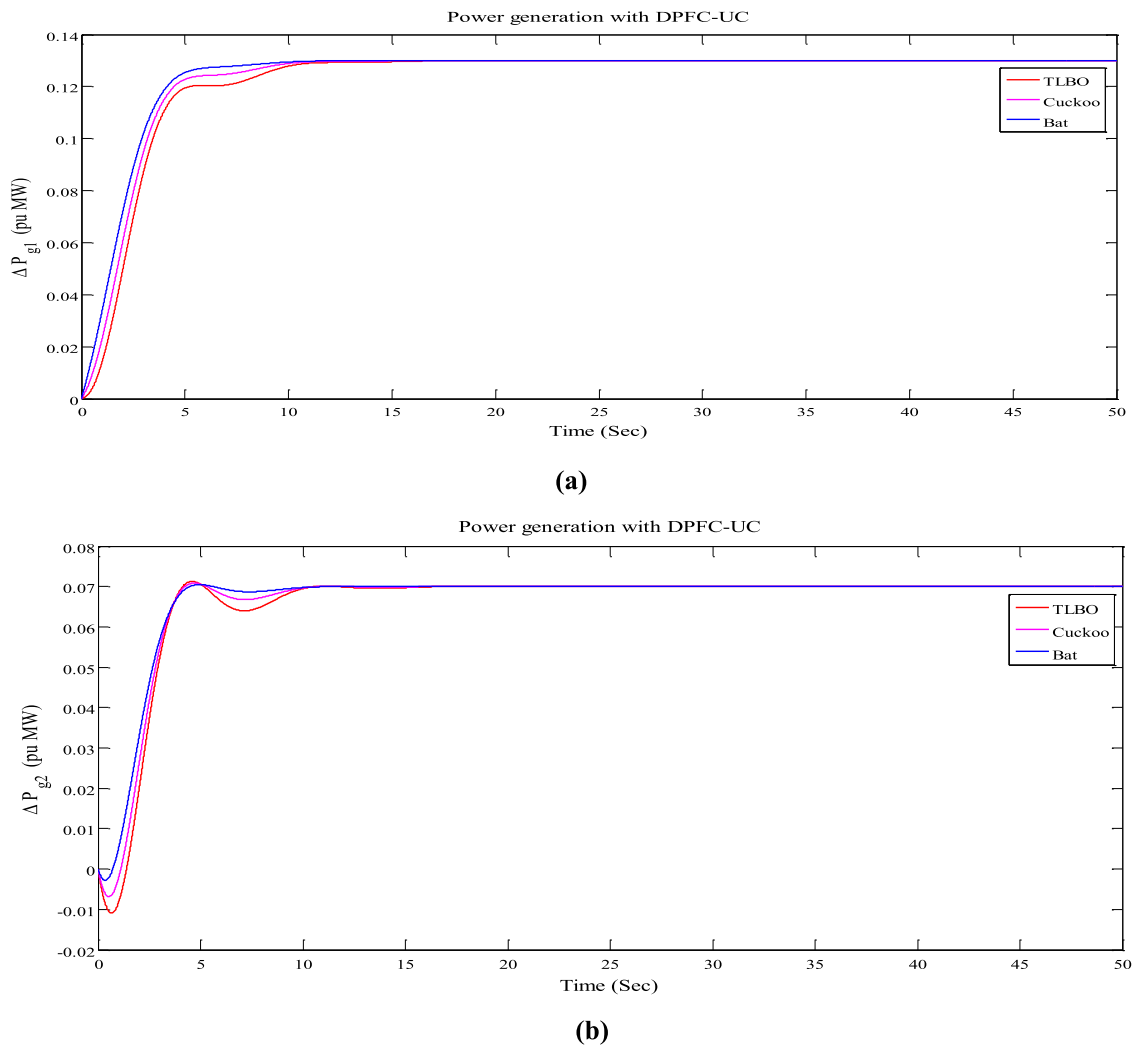
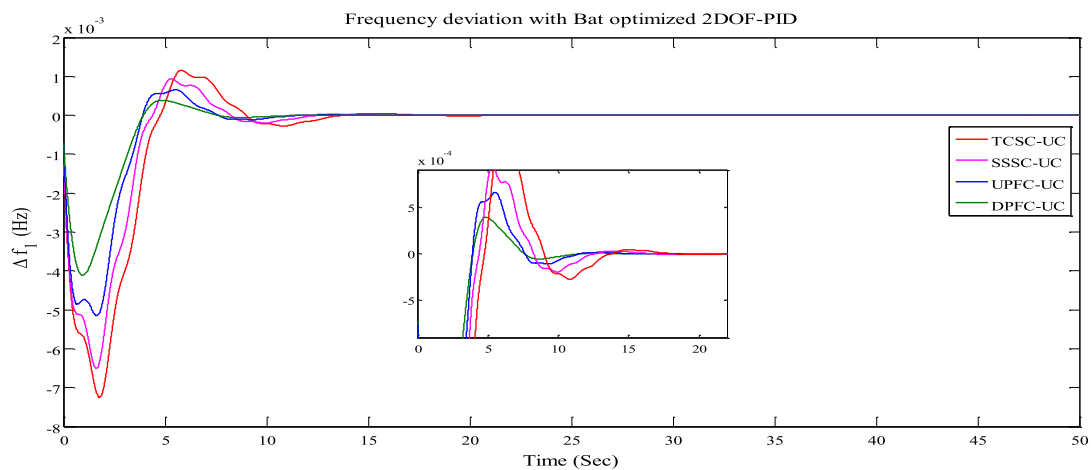
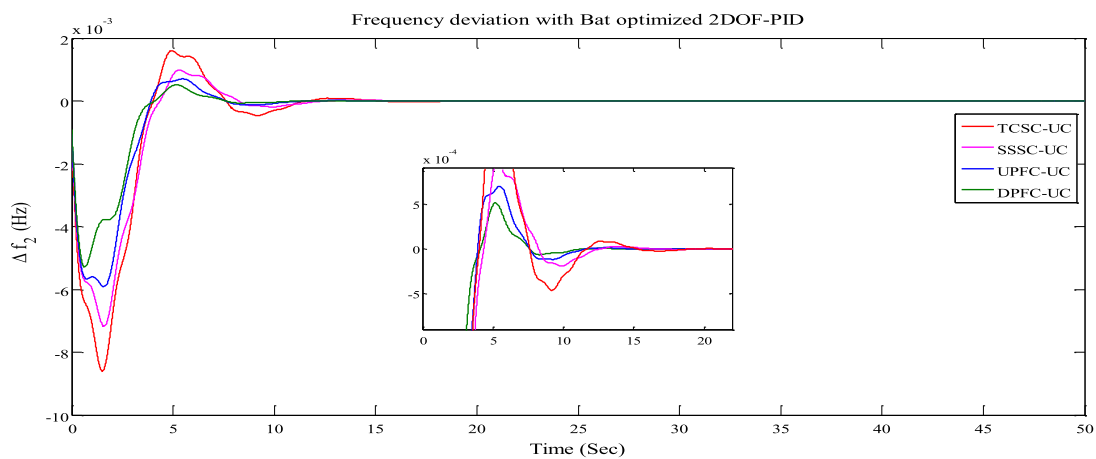


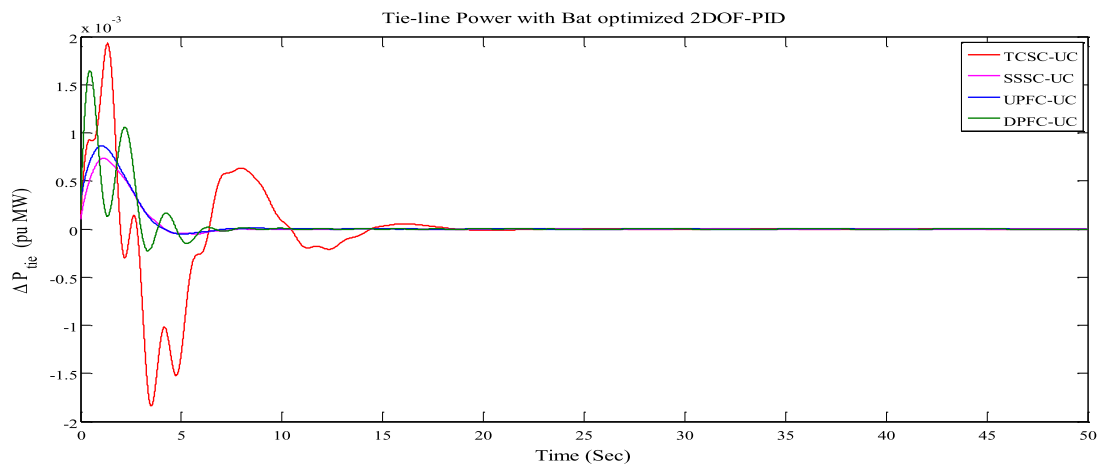
Fig. 15. Power generation with three algorithms of DPFC-UC.



(a)



(b)



(c)

Fig. 16. Frequency and tie-line power outcomes in bi-lateral case with FACTS-UC.

Table 10
Numerical data of ISE, ST, US, and OS in bilateral case with different compensators.

Control Approach	Response	OS	US	ST	ISE
Bat-2DOF-PID -TCSC-UC	ΔF_1	0.0017	-0.0075	17.15	0.0415
Bat-2DOF-PID -TCSC-UC	ΔF_2	0.0019	-0.0083	18.26	
Bat-2DOF-PID -TCSC-UC	ΔP_{tie}	0.0181	-0.0004	17.83	
Bat-2DOF-PID -SSSC-UC	ΔF_1	0.0011	-0.0067	13.27	0.0245
Bat-2DOF-PID -SSSC-UC	ΔF_2	0.0013	-0.0072	14.28	
Bat-2DOF-PID -SSSC-UC	ΔP_{tie}	0.0008	-0.00018	13.88	
Bat-2DOF-PID -UPFC-UC	ΔF_1	0.00075	-0.00057	12.81	0.0168
Bat-2DOF-PID -UPFC-UC	ΔF_2	0.00092	-0.00061	12.97	
Bat-2DOF-PID -UPFC-UC	ΔP_{tie}	0.00071	-0.00052	13.12	
Bat-2DOF-PID -DPFC-UC	ΔF_1	0.00051	-0.00039	11.54	0.0092
Bat-2DOF-PID -DPFC-UC	ΔF_2	0.00045	-0.00053	11.78	
Bat-2DOF-PID -DPFC-UC	ΔP_{tie}	0.00159	-0.00012	9.5	

combination of various FACTS controllers and UC in the presence of suggested optimization techniques. Moreover, the finer gains of the 2DOF-PID controller with coordination of FACTS controllers and UC is reported in Table 6. Likewise, the tie-line power variations with compensators are represented in Fig. 14(a)-(d). The performance analysis of the suggested methods has been reported in Table 7. It should be noted from the Table 7 that the performance indices of the bat optimized 2DOF PID with DPFC-UC (ISE=0.0362) is low as compared with the CS (ISE=0.045) and TLBO (ISE=0.108) tuned 2DOF PID with DPFC-UC. In order to find out the effectiveness of the suggested method, it has been compared with the recently existed studies, and reported in Table 8. As per the simulation outcomes, the bat optimized 2DOF-PID with coordination of DPFC and UC yields the productive outcomes with regards to ST, OS, US and enhances the system dynamic stability over studied methods. The bat optimized gains of the 2DOF-PID with the combination of DPFC and UC is mentioned in Table 9.

Fig. 15(a)-(b) represents the GENCOs generated power with three algorithms in the presence of DPFC-UC. As stated to (19), the produced power from GENCOs is $\Delta P_{G1} = 0.13$ pu MW, $\Delta P_{G2} = 0.07$ pu MW, $\Delta P_{G3} = \Delta P_{G4} = 0$ pu MW. It should be noted that the produced level of the GENCOs power is almost equal to their particular values, and which meets the load demand of the DISCOs in area 1. Since area 2 is not in contract mode for this transaction, their output power is reached to zero at steady state. Bat optimized 2DOF-PID with the combination of DPFC and UC contributes the satisfactory

GENCOs profile with regard to less settling time, undershoot and overshoot.

3.2. Bilateral transaction

In this case, all GENCOs and DISCOs should not have any restrictions for making the agreement between the areas. Moreover, DISCOs have greater opportunities to establish the contract with all GENCOs in the same area or other areas. The DPM matrix shows the power transaction of all DISCOs with all GENCOs and is represented in Equ. (37).

$$DPM = \begin{bmatrix} 0.1 & 0.24 & 0.33 & 0.18 \\ 0.2 & 0.16 & 0.17 & 0.22 \\ 0.27 & 0.4 & 0.5 & 0 \\ 0.43 & 0.2 & 0 & 0.6 \end{bmatrix} \quad (37)$$

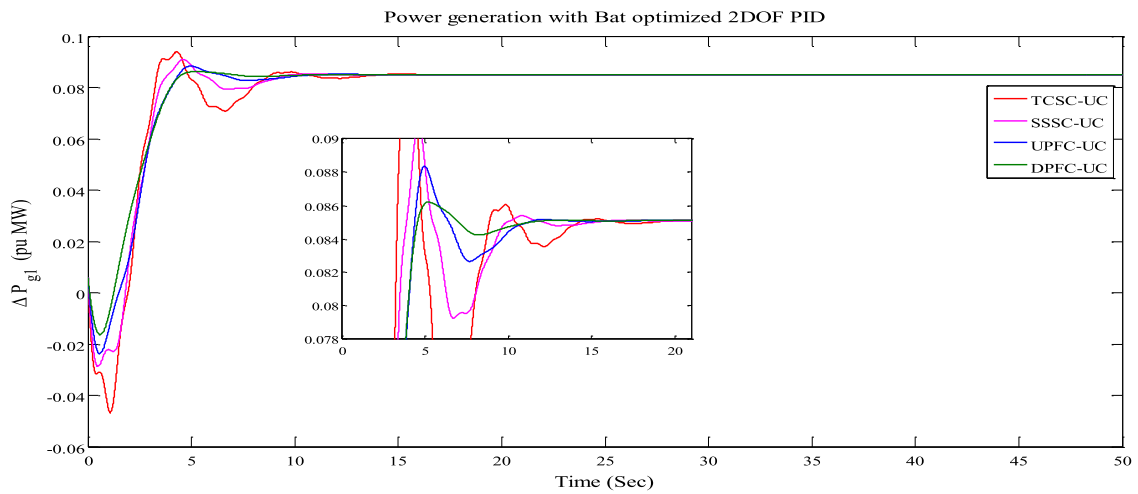
From matrix in (37), off-diagonal digits illustrated that the DISCOs made contract with another area GENCOs. The nominal steady state power between areas ($\Delta P_{tie, nom}$) is determined.

$$\Delta P_{tie, nom} = (0.33 + 0.17)X0.1 + (0.18 + 0.22)X0.1 - (0.27 + 0.43)X0.1 - (0.4 + 0.2)X0.1 = -0.041 \text{ pu MW} \quad (38)$$

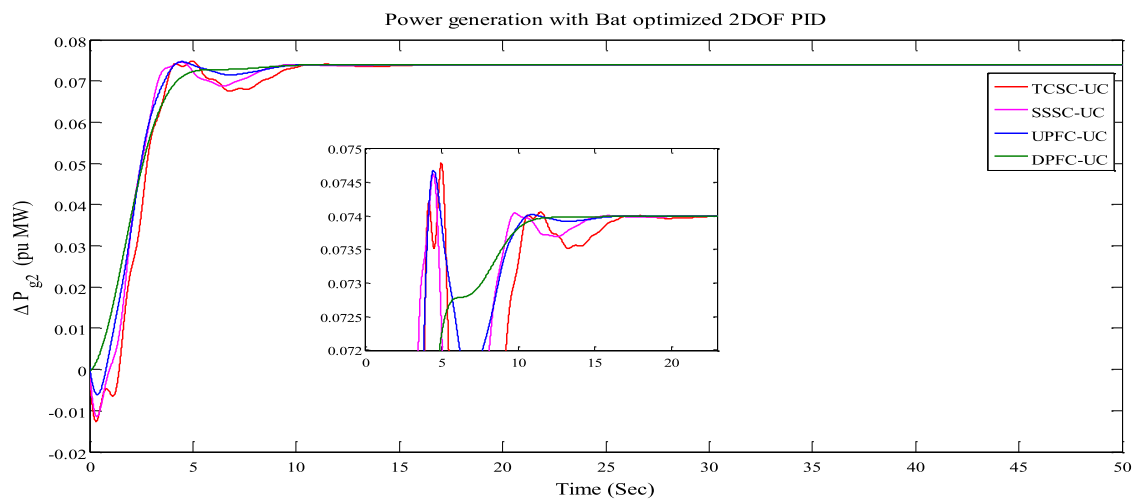
Fig. 16(a)-(c) indicates the frequency and tie-line power changes in bilateral case with various compensators of bat optimized 2DOF-PID. It should be noted that the UC and FACTS controllers like SSSC, TCSC, UPFC, and DPFC shows a remarkable performance for diminishing the

Table 11
Comparative performance of proposed method with existed studies in bilateral case.

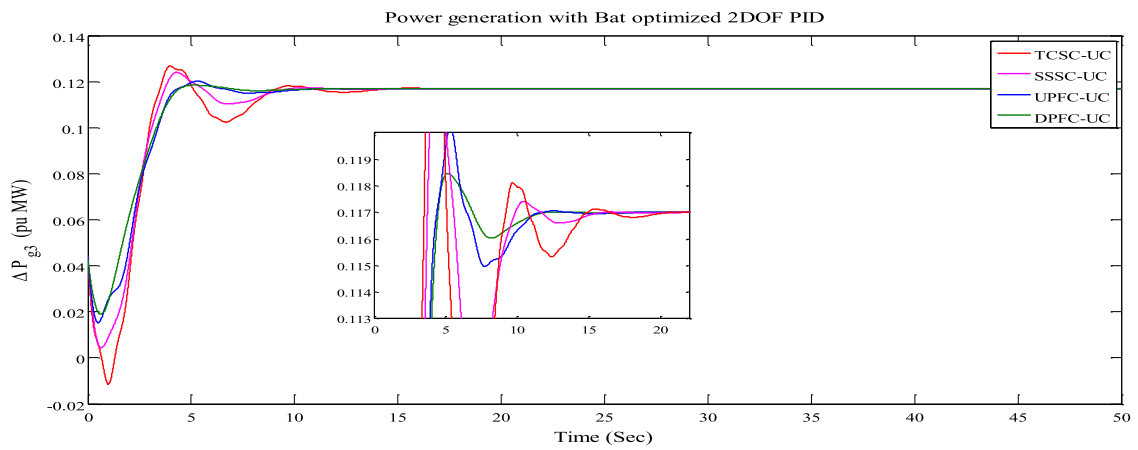
Controller type	Bilateral Overshoot (OS)			ISE
	ΔF_1	ΔF_2	ΔP_{tie}	
hTLBO-PS based TID with TCPS-SMES [21]	0.0599	0.0591	0.0164	0.666
DE-PID [12]	0.0988	0.0683	0.0524	0.4945
QOHS-TCSC-PID [23]	0.0041	0.0018	0.0833	0.0132
Proposed method (BAT optimized 2DOF PID with DPFC-UC)	0.00051	0.00045	0.00159	0.0092



(a)

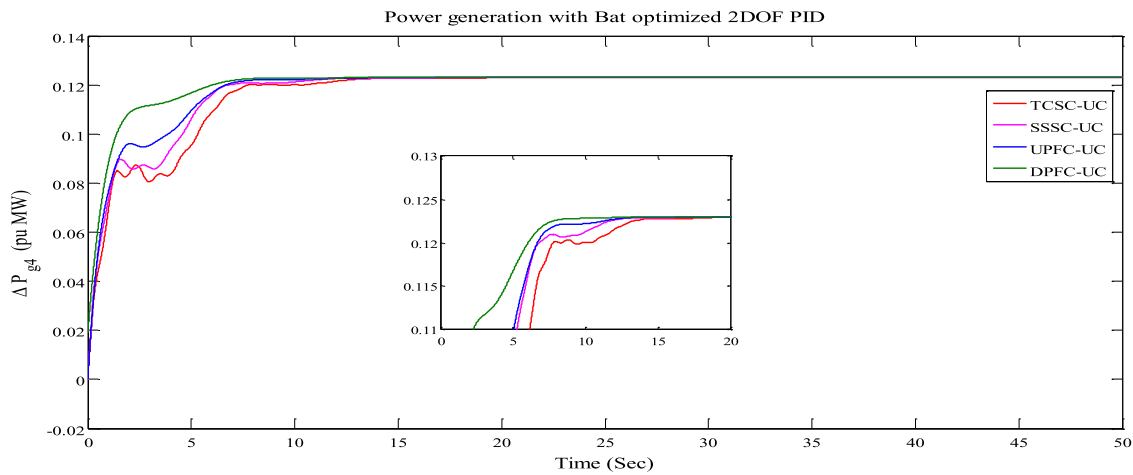


(b)



(c)

Fig. 17. Power generations with bat optimized 2DOF-PID of various compensators.



(d)

Fig. 17. (continued)

fluctuations in frequency and tie-line power. The numerical data of ISE, ST, US, and OS are recorded in Table 10. The simulation results disclose that the ST of frequency deviations in area 1 with bat tuned 2DOF PID in the presence of amalgamation of FACTS and UC are 17.15 s for TCSC-UC, 13.27 s for SSSC-UC, 12.81 s for UPFC-UC and 11.54 s for DPFC-UC. It has been observed that the bat tuned 2DOF PID with the combination of DPFC-UC shows less settling time and gives 32.17%, 13.03%, 9.91% enhancement than TCSC-UC, SSSC-UC, UPFC-UC respectively. For area 2, 18.26 s for TCSC-UC, 14.28 s for SSSC-UC, 12.97 s for UPFC-UC and 11.78 s for DPFC-UC. Similarly, for tie-line power, 17.83 s for TCSC-UC, 13.88 s for SSSC-UC, 13.12 s for UPFC-UC, 9.52 s for DPFC-UC. Furthermore, the indices value of the DPFC-UC (ISE=0.0092) is less over TCSC-UC (ISE=0.0415), SSSC-UC (ISE=0.0245), UPFC-UC (ISE=0.0168).

Moreover, the proposed bat tuned 2DOF PID with DPFC-UC has been contrasted with the other existed studies and recorded in Table 11. Eventually, the numerical data of this investigation demonstrate that the bat tuned 2DOF PID with DPFC-UC retains better dynamic performance in terms of ISE, ST, OS, US and enriches the system stability. The gain values of the 2DOF-PID controller with DPFC-UC is mentioned in Table 9.

Fig. 17(a)-(d) demonstrates the profile of GENCOs output power with different control techniques. As considered to (19), the GENCOs generated power profile is $\Delta P_{G1} = 0.0851$ pu MW, $\Delta P_{G2} = 0.075$ pu MW, $\Delta P_{G3} = 0.117$ pu MW, $\Delta P_{G4} = 0.123$ pu MW. From the Fig. 17(a)-(d), the GENCOs produced power is nearly attained to their scheduled values with the suggested methods and alleviated the variations in system. Thereby, the bat tuned 2DOF-PID with the

coordination of DPFC and UC shows better outcomes over other studied techniques.

3.3. Contract violation

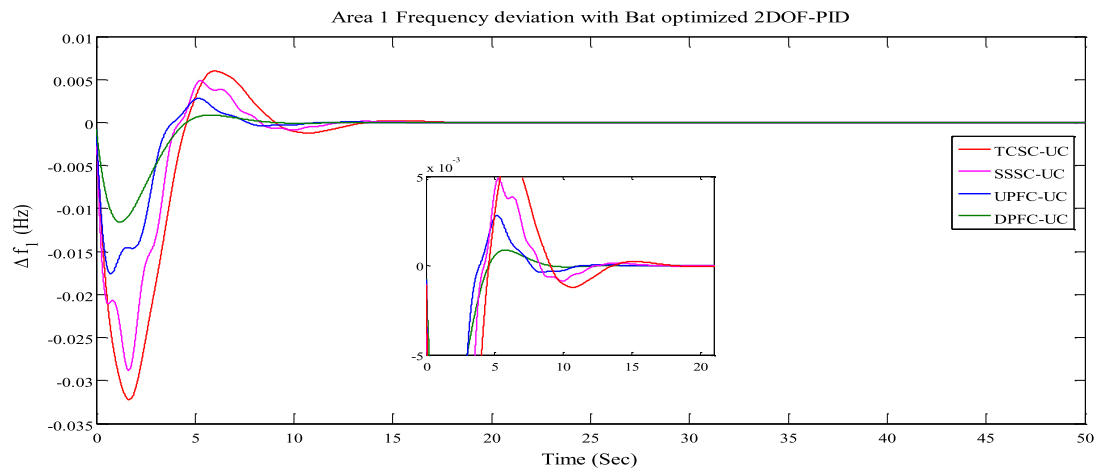
In this transaction, the loads of the DISCO have got surplus power, it is not favourable to agreement ethics. In addition, the surplus load power is reflected as an internal load of that regional area. The GENCOs must be delivered the uncontracted power of the own area as the DISCOs. In this regard, the DISCO 1 surplus load demand is considered as 0.10 pu MW.

Therefore, the total demand on area 1 is:

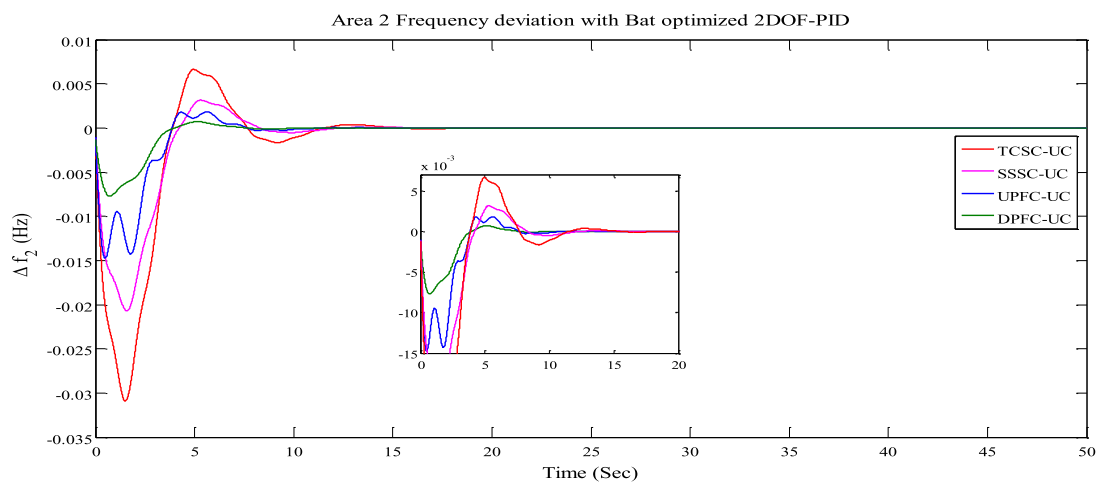
$$\begin{aligned} \Delta P_{d1} &= \text{DISCO 1 contracted load} + \text{DISCO 2 contracted load} \\ &\quad + \text{uncontracted load} \\ &= 0.10 + 0.10 + 0.10 = 0.30 \text{ pu MW} \end{aligned}$$

Fig. 18(a)-(c) depicts the frequency and tie-line power oscillations mitigations with bat tuned 2DOF-PID in the presence of distinct compensators. The performance analysis of the dynamic responses is indicated in Table 12. Based on the results, the settling time of dynamic responses of ΔF_1 , ΔF_2 , ΔP_{tie} are 9.87 s, 7.24 s, 9.65 s for DPFC-UC whereas, 16.31 s, 15.25 s, 16.28 s for TCSC-UC, 13.82 s, 12.73 s, 11.88 s for SSSC-UC, 10.81 s, 8.93 s, 10.21 s for UPFC-UC respectively. It has been observed that the combination of DPFC and UC exhibits the less settling time and strengthens the dynamic stability of the system.

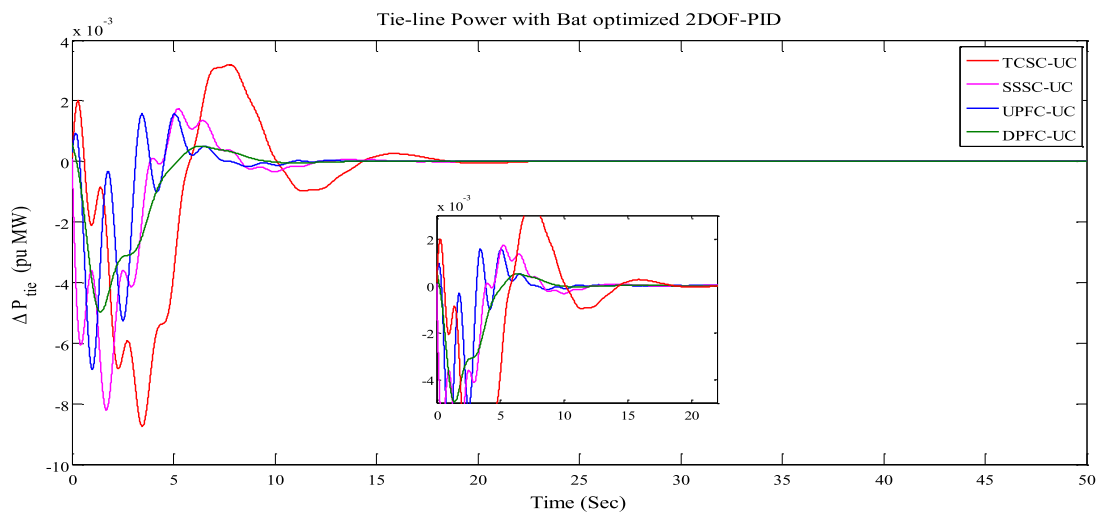
Besides, the amalgamation of DPFC and UC contributes minimum



(a)



(b)



(c)

Fig. 18. Frequency and tie-line power changes with distinct compensator in contract violation.

Table 12
Performance analysis of compensators with bat optimized 2DOF-PID under contract violation.

Control Approach	Response	OS	US	ST	ISE
Bat-2DOF-PID -TCSC-UC	ΔF_1	0.0067	-0.0519	16.31	0.357
Bat-2DOF-PID -TCSC-UC	ΔF_2	0.0073	-0.0464	15.25	
Bat-2DOF-PID -TCSC-UC	ΔP_{tie}	0.0037	-0.0084	16.28	
Bat-2DOF-PID -SSSC-UC	ΔF_1	0.0051	-0.0445	13.82	0.182
Bat-2DOF-PID -SSSC-UC	ΔF_2	0.0042	-0.0337	12.73	
Bat-2DOF-PID -SSSC-UC	ΔP_{tie}	0.0019	-0.0078	11.88	
Bat-2DOF-PID -UPFC-UC	ΔF_1	0.0029	-0.0166	10.81	0.0645
Bat-2DOF-PID -UPFC-UC	ΔF_2	0.0015	-0.0142	8.93	
Bat-2DOF-PID -UPFC-UC	ΔP_{tie}	0.0011	-0.0062	10.21	
Bat-2DOF-PID -DPFC-UC	ΔF_1	0.0007	-0.0125	9.87	0.0287
Bat-2DOF-PID -DPFC-UC	ΔF_2	0.0001	-0.0058	7.24	
Bat-2DOF-PID -DPFC-UC	ΔP_{tie}	0.0008	-0.0048	9.65	

Table 13
Comparative analysis of proposed method with existed methods in contract violation.

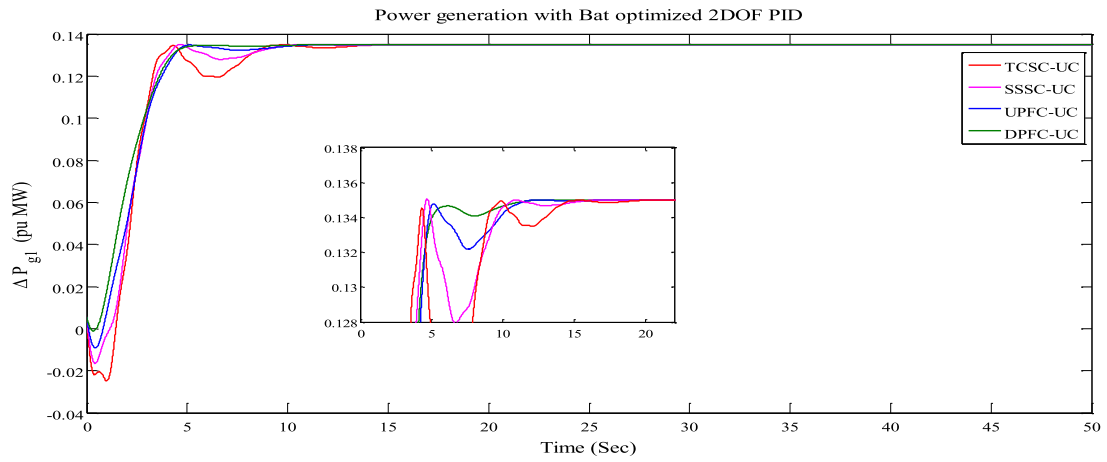
Controller type	Contract violation Overshoot (OS)			ISE
	ΔF_1	ΔF_2	ΔP_{tie}	
hTLBO-PS based TID with TCPS-SMES [21]	0.0231	0.0352	0.0390	1.8352
DE-PID [12]	0.1093	0.0641	0.0521	0.7605
Proposed method (BAT optimized 2DOF PID with DPFC-UC)	0.0007	0.0001	0.0008	0.0287

performance indices (ISE=0.028) value as compared with TCSC-UC (ISE = 0.357), SSSC-UC (ISE = 0.182), UPFC-UC (ISE = 0.064). In order to determine the productive assessment of the suggested approach, it has been contrasted with the previous studies and mentioned in Table 13. Finally, the results disclose that the bat tuned 2DOF PID with the amalgamation of DPFC and UC show the finest dynamic performance than other approaches. The bat optimized optimal values of the 2DOF-PID with DPFC-UC is reported in Table 9.

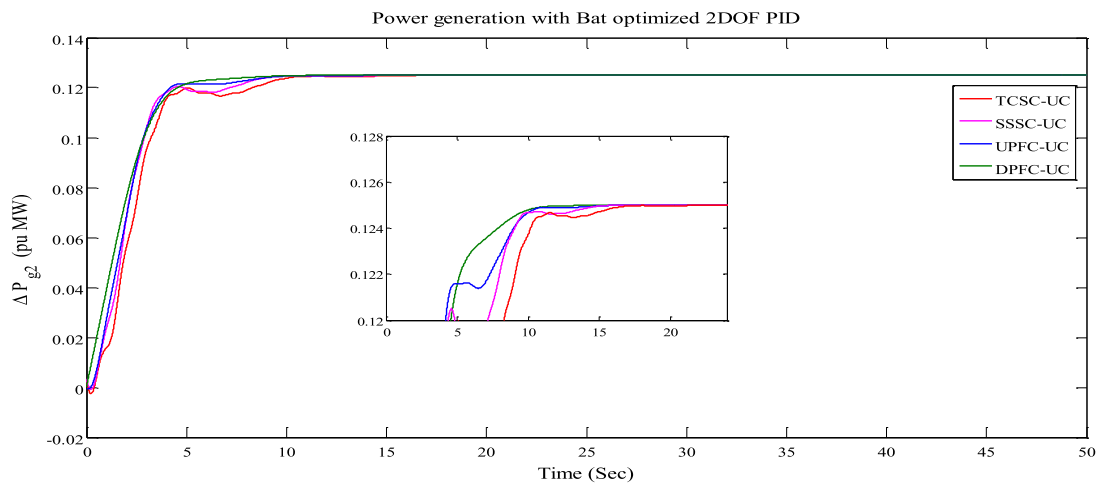
The profile of GNECOs produced power is the significant discussion in this agreement due to presence of uncontracted load. It has been represented in Fig. 19(a)-(d). The GNECOs generated power profile is $\Delta P_{G1} = 0.135$ pu MW, $\Delta P_{G2} = 0.125$ pu MW, $\Delta P_{G3} = 0.117$ pu MW, $\Delta P_{G4} = 0.123$ pu MW. Based on the simulation results, the uncontracted load demand of DISCO 1 is met by GENCO 1 and GENCO 2 only. It should be noted that the uncontracted load of DISCO 1 is not influenced the GENCO 3 and GENCO 4 powers.

4. Conclusion

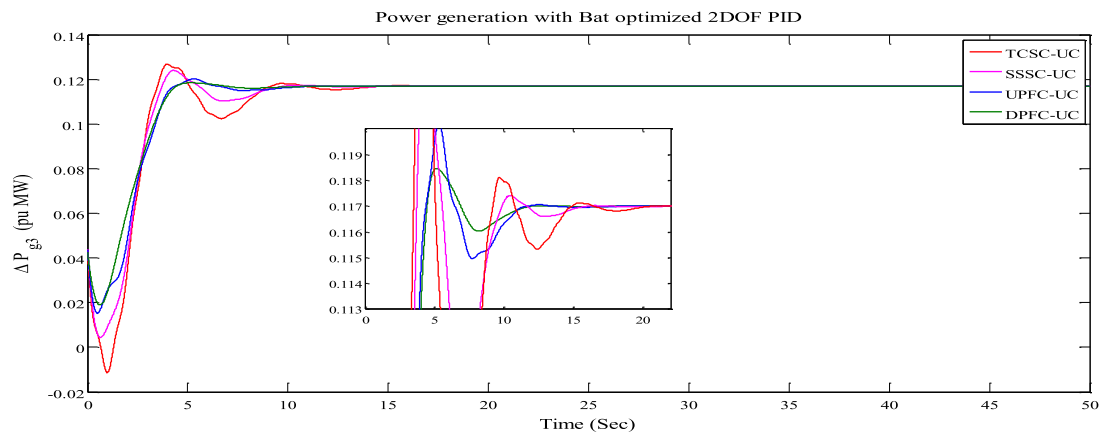
In this study, AGC of two-area diverse sources of interconnected system has investigated with different control methods under liberalized environment. Three distinct optimization techniques such as cuckoo, TLBO, and bat algorithm are utilized to acquire the optimal gain values of the PID/2DOF PI/2DOF PID controllers. Moreover, the combination of ultra-capacitor (UC) and sophisticated FACTS controllers like SSSC, UPFC, TCSC, and DPFC are integrated to the two-area restructured system for strengthening the system stability. An attempt has been made to introduce the DPFC for the first time in the AGC of deregulated system. The simulation results disclose that the bat optimized 2DOF-PID with the combination of UC and DPFC gave prolific dynamic performances as compared with other studied methods. Moreover, it has been shown less settling time, stabilized the oscillations as rapidly as possible, and enhanced the system performance.



(a)

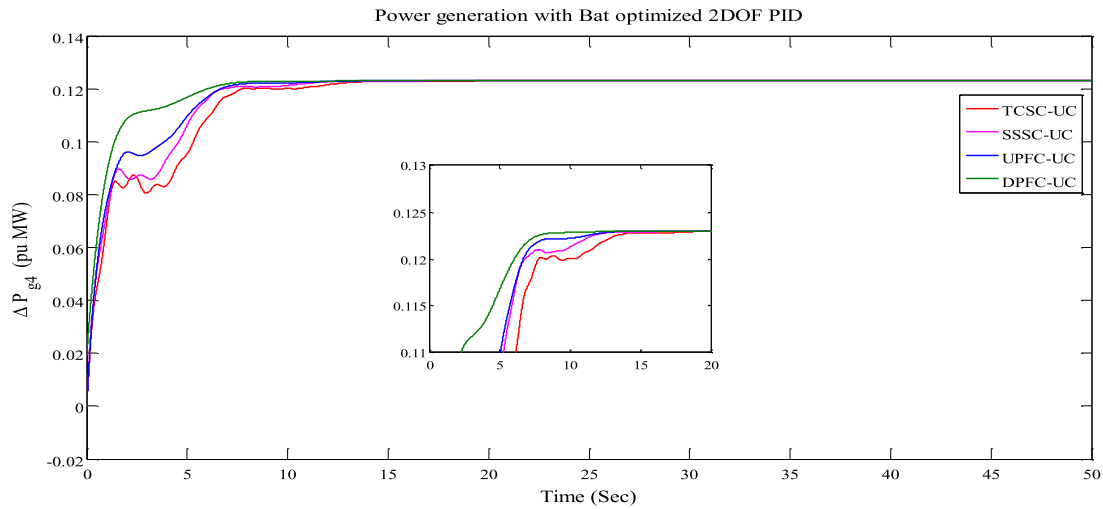


(b)



(c)

Fig. 19. Power generation in contract violation with bat optimized compensators.



(d)

Fig. 19. (continued)

AUTHORSHIP STATEMENT

All persons who meet authorship criteria are listed as authors, and all authors certify that they have participated sufficiently in the work to take responsibility for the content, including participation in the concept, design, analysis, writing, or revision of the manuscript. Furthermore, each author certifies that this material or similar material has not been published elsewhere, accepted for publication elsewhere or under editorial review for publication elsewhere.

Authorship contributions

K. Peddakapu: Main Author. Acquisition of data, drafting the manuscript, analysis and/or interpretation of data, revising the manuscript, approval the version of manuscript to be published

M. R. Mohamed: Corresponding Author. Conception and design of study, analysis and/or interpretation of data, revising the manuscript critically for important intellectual content, approval the version of manuscript to be published

M.H. Sulaiman: Grant Funding. Analysis and/or interpretation of data, revising the manuscript critically for important intellectual

content, approval the version of manuscript to be published

P. Srinivasarao: Revising the manuscript critically for important intellectual content, approval the version of manuscript to be published

A.S. Veerendra: Analysis and/or interpretation of data, revising the manuscript critically for important intellectual content, approval the version of manuscript to be published

P.K. Leung: Revising the manuscript critically for important intellectual content, approval the version of manuscript to be published

Declaration of Competing Interest

The authors declare that they have no known competing financial interests or personal relationships that could have appeared to influence the work reported in this paper.

Funding Acknowledgement

This project is supported by Universiti Malaysia Pahang (UMP). Mr. K. Peddakapu is working under UMP's Doctoral Research Scheme (DRS) and part of UMP's internal grant RDU1803101.

Appendix

System Specifications	$f = 60 \text{ Hz}$, Each area power rating = 1200MW, Base power = 1200MW.
Power plant details	$T_{g1} = 0.08 \text{ s}$, $T_{i1} = 0.3 \text{ s}$, $K_{PS1} = K_{PS2} = 120 \frac{\text{Hz}}{\text{pu}}$, $T_{PS1} = 6$, $T_{PS2} = 0.041$, $R_1 = R_2 = R_3 = R_4 = 2.4 \frac{\text{Hz}}{\text{pu}}$,
FACTS controllers and ultracapacitor data	$B_1 = B_2 = 0.425 \text{ pu} \frac{\text{MW}}{\text{Hz}}$, $T_{R1} = T_{R2} = 0.513 \text{ s}$, $T_1 = T_2 = T_3 = T_4 = 10 \text{ s}$, $K_1 = K_2 = 0.333$, $2\pi T_{12} = 0.545 \text{ pu} \frac{\text{MW}}{\text{Hz}}$, $a_{12} = a_{21} = -1$, $T_{W1} = T_{W2} = 1 \text{ s}$, $T_{dg} = 0.1 \text{ s}$, $T_{dt} = 8 \text{ s}$, $K_p = 1.25$, $K_{p2} = 1.4$, $K_1 = 0.85$. $T_{TCSC} = 0.015 \text{ s}$, $T_{SSSC} = 0.31 \text{ s}$, $T_{UPFC} = 0.01 \text{ s}$, $T_{DPFC} = 0.008 \text{ s}$, $K_{TCSC} = 1$, $K_{SSSC} = 0.1802$, $K_{UPFC} = 0.01$, $K_{DPFC} = 1$, $T_{UCi} = 0.9 \text{ s}$, $K_{UCi} = -7/10$.
Liberalization power system details	Area control error (ACE) participation attributes: $apf_1 = apf_2 = apf_3 = apf_4 = 0.5$, $\Delta P_{DISCO1} = \Delta P_{DISCO2} = 0.1 \text{ pu} = \Delta P_{DISCO3} = \Delta P_{DISCO4}$.

References

- [1] N. Jaleeli, L.S. VanSlyck, D.N. Ewart, L.H. Fink, A.G. Hoffmann, Understanding automatic generation control, *IEEE Trans. power Syst.* 7 (3) (1992) 1106–1122.
- [2] S. Saxena, Y.V. Hote, Load frequency control in power systems via internal model control scheme and model-order reduction, *IEEE Trans. power Syst.* 28 (3) (2013) 2749–2757.
- [3] M. Rezasudin Basir Khan, Jagadeesh Pasupuleti, Razali Jidin, Load frequency control for mini-hydropower system: a new approach based on self-tuning fuzzy proportional-derivative scheme, *Sustainable Eng. Tech. and Asst.* 30 (2018) 253–262.
- [4] H. Shayeghi, H.A. Shayanfar, O.P. Malik, Robust decentralized neural networks based LFC in a deregulated power system, *Electr. Power Syst. Res.* 77 (3–4) (2007) 241–251.
- [5] S. Debbarma, L.C. Saikia, N. Sinha, AGC of a multi-area thermal system under deregulated environment using a non-integer controller, *Electr. Power Syst. Res.* 95 (2013) 175–183.
- [6] L.C. Saikia, J. Nanda, S. Mishra, Performance comparison of several classical controllers in AGC for multi-area interconnected thermal system, *Int. J. Electr. Power Energy Syst.* 33 (3) (2011) 394–401.
- [7] R.K. Sahu, S. Panda, U.K. Rout, DE optimized parallel 2-DOF PID controller for load frequency control of power system with governor dead-band nonlinearity, *Int. J. Electr. Power Energy Syst.* 49 (2013) 19–33.
- [8] R.K. Sahu, S. Panda, U.K. Rout, D.K. Sahoo, Teaching learning based optimization algorithm for automatic generation control of power system using 2-DOF PID controller, *Int. J. Electr. Power Energy Syst.* 77 (2016) 287–301.
- [9] J. Sánchez, A. Visioli, S. Dormido, A two-degree-of-freedom PI controller based on events, *J. Process Control* 21 (4) (2011) 639–651.
- [10] H. Shabani, B. Vahidi, M. Ebrahimpour, A robust PID controller based on imperialist competitive algorithm for load-frequency control of power systems, *ISA Trans.* 52 (1) (2013) 88–95.
- [11] H. Guolian, Q. Lina, Z. Xinyan, Z. Jianhua, Application of PSO-based fuzzy PI controller in multi-area AGC system after deregulation, 2012 7th IEEE Conference on Industrial Electronics and Applications (ICIEA), 2012, pp. 1417–1422.
- [12] P.K. Hota, B. Mohanty, Automatic generation control of multi-source power generation under deregulated environment, *Int. J. Electr. Power Energy Syst.* 75 (2016) 205–214.
- [13] S. Debbarma, L.C. Saikia, Bacterial foraging based FOPID controller in AGC of an interconnected two-area reheat thermal system under deregulated environment, *IEEE-International Conference On Advances In Engineering, Science And Management (ICAESM-2012)*, 2012, pp. 303–308.
- [14] T.S. Gorripotu, R.K. Sahu, S. Panda, Application of firefly algorithm for AGC under deregulated power system, *Computational Intelligence in Data Mining-Volume 1*, Springer, 2015, pp. 677–687.
- [15] S. Dhundhara, Y.P. Verma, Capacitive energy storage with optimized controller for frequency regulation in realistic multisource deregulated power system, *Energy* 147 (2018) 1108–1128.
- [16] B.K. Sahu, S. Pati, P.K. Mohanty, S. Panda, Teaching–learning based optimization algorithm based fuzzy-PID controller for automatic generation control of multi-area power system, *Appl. Soft Comput.* 27 (2015) 240–249.
- [17] A.S. Oshaba, E.S. Ali, S.M. Abd Elazim, MPPT control design of PV system supplied SRM using BAT search algorithm, *Sustainable Eng. Grid & Netw* 2 (2015) 51–60.
- [18] Y. Arya, N. Kumar, S.K. Gupta, Optimal automatic generation control of two-area power systems with energy storage units under deregulated environment, *J. Renew. & Sust. Eng.* 9 (2017).
- [19] A. Saha, L.C. Saikia, Performance analysis of combination of ultra-capacitor and superconducting magnetic energy storage in a thermal-gas AGC system with utilization of whale optimization algorithm optimized cascade controller, *J. Renew. & Sust. Eng.* 10 (2018).
- [20] P. Dash, L.C. Saikia, N. Sinha, Comparison of performances of several FACTS devices using cuckoo search algorithm optimized 2DOF controllers in multi-area AGC, *Int. J. Electr. Power Energy Syst.* 60 (2015) 316–324.
- [21] D. Khamari, R.K. Sahu, T.S. Gorripotu, S. Panda, Automatic generation control of power system in deregulated environment using hybrid TLBO and pattern search technique, *Ain Shams Eng. J.* (2019).
- [22] M. Nandi, C.K. Shiva, V. Mukherjee, Frequency stabilization of multi-area multi-source interconnected power system using TCSC and SMES mechanism, *J. Energy Storage* 14 (2017) 348–362.
- [23] M. Nandi, C.K. Siva, V. Mukherjee, TCSC based automatic generation control of deregulated power system using quasi-oppositional harmony search algorithm, *Eng. Sci. Technol. an Int. J.* 20 (2017) 1380–1395.
- [24] R.K. Sahu, T.S. Gorripotu, S. Panda, A hybrid DE–PS algorithm for load frequency control under deregulated power system with UPFC and RFB, *Ain Shams Eng. J.* 6 (3) (2015) 893–911.
- [25] D. Das, S.K. Aditya, D.P. Kothari, Dynamics of diesel and wind turbine generators on an isolated power system, *Int. J. Electr. Power Energy Syst.* 21 (3) (1999) 183–189.
- [26] S. Panda, Multi-objective evolutionary algorithm for SSSC-based controller design, *Electr. Power Syst. Res.* 79 (6) (2009) 937–944.